(1

The Effect of Water Content on the Predictions of the Cloud Rise Module of DELFIC

Bryan M. Minor
Second Lieutenant, USAF

AFIT/GNE/ENP/88M-7

DEPARTMENT OF THE AIR FORCE
AIR UNIVERSITY
AIR FORCE INSTITUTE OF TECHNOLOGY

Wright-Patterson Air Force Base, Ohio

UNCLASSIFIED
SECURITY CLASSIFICATION OF THIS PAGE

REPORT DOCUMENTATION PAGE

Form Approved OMB No. 0704-0188

1a. REPORT SECURITY CLASSIFICATION: UNCLASSIFIED	1b. RESTRICTIVE MARKINGS
2a. SECURITY CLASSIFICATION AUTHORITY	3. DISTRIBUTION/AVAILABILITY OF REPORT: Approved for public release; distribution unlimited.
2b. DECLASSIFICATION/DOWNGRADING SCHEDULE	
4. PERFORMING ORGANIZATION REPORT NUMBER(S): AFIT/GNE/ENP/88M-7	5. MONITORING ORGANIZATION REPORT NUMBER(S)
6a. NAME OF PERFORMING ORGANIZATION: School of Engineering; 6b. OFFICE SYMBOL (If applicable): AFIT/ENP	7a. NAME OF MONITORING ORGANIZATION
6c. ADDRESS (City, State, and ZIP Code): Air Force Institute of Technology, Wright-Patterson AFB OH 45433-6583	7b. ADDRESS (City, State, and ZIP Code)
8a. NAME OF FUNDING/SPONSORING ORGANIZATION; 8b. OFFICE SYMBOL (If applicable)	9. PROCUREMENT INSTRUMENT IDENTIFICATION NUMBER
8c. ADDRESS (City, State, and ZIP Code)	10. SOURCE OF FUNDING NUMBERS: PROGRAM ELEMENT NO. / PROJECT NO. / TASK NO / WORK UNIT ACCESSION NO.

11. TITLE (Include Security Classification)
See box 19

12. PERSONAL AUTHOR(S)
Bryan M. Minor, B.S., 2d Lt, USAF

13a. TYPE OF REPORT	13b. TIME COVERED	14. DATE OF REPORT (Year, Month, Day)	15. PAGE COUNT
MS Thesis	FROM ____ TO ____	1988 March	97

16. SUPPLEMENTARY NOTATION

17. COSATI CODES FIELD	GROUP	SUB-GROUP
19	11	

18. SUBJECT TERMS (Continue on reverse if necessary and identify by block number)
Nuclear Clouds, Nuclear Explosion Simulation

19. ABSTRACT (Continue on reverse if necessary and identify by block number)

Title: THE EFFECT OF WATER CONTENT ON THE PREDICTIONS OF THE CLOUD RISE MODULE OF DELFIC

Thesis Chairman: Charles J. Bridgman, PhD
Professor of Nuclear Engineering

Approved for public release: IAW AFR 190-1.
LYNN E. WOLAVER 15 Jul 88
Dean for Research and Professional Development
Air Force Institute of Technology (AU)
Wright-Patterson AFB OH 45433

20. DISTRIBUTION/AVAILABILITY OF ABSTRACT: ☐ UNCLASSIFIED/UNLIMITED ☒ SAME AS RPT. ☐ DTIC USERS	21. ABSTRACT SECURITY CLASSIFICATION: UNCLASSIFIED
22a. NAME OF RESPONSIBLE INDIVIDUAL: Charles J. Bridgman, PhD	22b. TELEPHONE (Include Area Code): (513)255-3576; 22c. OFFICE SYMBOL: AFIT/ENP

DD Form 1473, JUN 86 — Previous editions are obsolete.

SECURITY CLASSIFICATION OF THIS PAGE
UNCLASSIFIED

(19)

The effect of water content on the predictions of the Cloud Rise Module, CRM, of the Defense Land Fallout Information Code, DELFIC, was examined. Problems with the theory of the CRM were found, especially how it handled the cloud's water content. The source code of the CRM was also found to have some contradictions with its documentation. All of the problems found with the CRM were addressed and a new version of DELFIC was created. This new version was then used to examine the predicted cloud height and volume for different humidity profiles and surface water mass loading of the cloud. Increasing the atmospheric humidity resulted in a lower stabilized cloud top and a smaller cloud volume. The effect of soil loading was also examined, and it was found to produce only slight changes in the stabilized cloud top and volume. The results found with the revised CRM were also compared to the results found using the original CRM. Both versions followed the same trends as the humidity profiles were changed, but the results found for the surface water loading case were very divergent. The differences in the results of the two versions suggest the results of the revised CRM are more valid.

1

AFIT/GNE/ENP/88M-7

The Effect of Water Content on the Predictions of the Cloud Rise Module of DELFIC

Bryan M. Minor
Second Lieutenant, USAF

AFIT/GNE/ENP/88M-7

1

AFIT/GNE/ENP/88M-7

THE EFFECT OF WATER CONTENT ON THE PREDICTIONS OF THE CLOUD RISE MODULE OF DELFIC

THESIS

Presented to the Faculty of the School of Engineering

of the Air Force Institute of Technology

Air University

In Partial Fulfillment of the

Requirements for the Degree of

Master of Science in Nuclear Science

Bryan M. Minor, B.S.

Second Lieutenant, USAF

January 1988

Preface

The purpose of this study was to examine the effect of water content on the predictions of the CRM of DELFIC. The emphasis of this study was on how it handles ambient water vapor and condensed water. A number of problems with the CRM were found and solutions to these problems proposed. The revised version of the CRM was then compared to the original version.

I have received a great deal of much needed help and guidance from my faculty advisor, Dr. Charles J. Bridgeman. The gracious help of Hillyer G. Norment was greatly appreciated. Also, I am thankful to my wife [redacted] for her understanding and much needed assistance in preparing this thesis.

Bryan M. Minor

Table of Contents

List of Figures

List of Tables

List of Symbols

$C_p(T)$ = weighted specific heat of dry air and atmospheric water vapor (J/(kg*K))

$$C_p(T) = (C_{pa}(T) + x*C_{pw}(T))/(1.0 + x)$$

$C_{pv}(T)$ = weighted specific heat of the cloud for the dry case (J/(kg*K))

$$C_{pv}(T) = \beta'*C_p(T) + (1-\beta')*C_s(T)*k(T,T_{si})$$

where: $k(T,T_{si}) = 1$ if $T_{si} >= T$

$k(T,T_{si}) = 0$ if $T_{si} < T$

$C_{pa}(T)$ = specific heat of dry air (J/(kg*K))

$C_{pw}(T)$ = specific heat of water (J/(kg*K))

$C_s(T)$ = specific heat of soil (J/(kg*K))

D_p = diameter of particle (m)

D_{sj} = mean soil particle diameter in the jth group (m)

D_{wj} = mean water particle diameter in the jth group (m)

E = turbulent kinetic energy density per unit mass (J)

E_{aw} = total energy used to heat dry air, atmospheric water vapor, and surface water (J)

$$E_{aw} = 0.45*Y - \int_{T_{ei}}^{T_{si}} C_s(T)dT$$

where: 0.45 = fraction of the yield energy

initially in the fireball

Y = weapon's yield energy (J)

f_j = terminal velocity of a particle in the jth size group (m/sec)

g = acceleration due to gravity (m/sec)

g = 9.8 (m/sec)

H_c = vertical radius of the cloud (m)

K_2 = dimensionless empirical parameter, used in the eddy viscosity term

K_3 = dimensionless empirical parameter, used in the energy dissipation term

L = latent heat of water,vaporization or ice (J/kg)

M = mass of the cloud (kg)

M_{ai} = initial air mass of the cloud (kg)

M_g = mass of the gases contained in the cloud, dry air and atmospheric water vapor (kg)

M_{wi} = initial water mass of the cloud (kg)

$(dM/dt)_{ent}$ = change of the entrained cloud mass with respect to time (kg/sec)

N_d = Davies number

$n_s(t)_j$ = the number of soil particles in the jth group per unit volume of the cloud (1/m^3)

$n_w(t)_j$ = the number of water particles in the jth group per unit volume of the cloud (1/m^3)

P = pressure (Pa)

$P(t)$ = total mass fallout rate from the cloud (kg/sec)

$P_s(t)$ = soil mass fallout rate from the cloud (kg/sec)

$P_w(t)$ = water mass fallout rate from the cloud (kg/sec)

R_a = ideal gas constant = 287. (J/(kg*K))

R_c = horizontal cloud radius (m)

s = soil mixing ratio = the ratio of the mass of soil to the unit mass of dry air containing it.

S = area (m^2)

S = 4*PI*R

where: PI = 3.1415927

t = time (sec)

T = cloud temperature (K)

T_e = ambient temperature at the cloud center altitude (K)

T_{ei} = initial ambient temperature at the cloud center altitude (K)

T_{ev} = ambient virtual temperature (K)

$$T_{ev} = T_e*(1 + x_e/\epsilon)/(1 + x_e)$$

T_i = initial cloud temperature (K)

T_{si} = initial soil temperature of the cloud (K)

T_v = cloud virtual temperature (K)

$$T_v = T*(1 + x/\epsilon)/(1 + x)$$

u = cloud vertical velocity (m/sec)

v = cloud's characteristic velocity (m/sec)

$$v = \max[\ |u|,\ (2*E)^{0.5}\ ]$$

V = cloud volume (m^3)

w = water mixing ratio = the ratio of the mass of water to the unit mass of dry air containing it.

W = weapon's yield (Kt)

x = water vapor mixing ratio in the cloud

x_e = atmospheric water vapor mixing ratio at the cloud center altitude

β' = ratio of the cloud's atmospheric water vapor and dry air density to its total density

$$\beta' = (1 + x)/(1 + x + w + s)$$

ϵ = ratio of molecular weights of water and air

$$\epsilon = (18.0 / 29.0)$$

ε = energy dissipation rate (J/(kg*sec))

μ = dimensionless empirical constant used in entrainment equation

η = dynamic viscosity of the cloud gas (kg/(m*sec))

ρ = density of the cloud (kg/m^3)

ρ_p = density of a particle (kg/m^3)

ρ_{ps} = density of a soil particle (kg/m^3)

ρ_{pw} = density of a water particle (kg/m^3)

ϕ = ratio of the energy used to heat dry air and

atmospheric water vapor to the energy used to heat surface water, atmospheric water vapor, and dry air

$$\phi = E_{a,wv} / (E_{a,wv} + E_{cw})$$

where: $E_{a,wv}$ = energy used to dry air and atmospheric water vapor (J)

E_{cw} = energy used to heat surface water (J)

Abstract

The effect of water content on the predictions of the Cloud Rise Module, CRM, of the Defense Land Fallout Information Code, DELFIC, was examined. Problems with the theory of the CRM were found, especially how it handled the cloud's water content. The source code of the CRM was also found to have some contradictions with its documentation. All of the problems found with the CRM were addressed and a new version of DELFIC was created. This new version was then used to examine the predicted nuclear cloud height and volume for different humidity profiles and surface water mass loading of the cloud. Increasing the atmospheric humidity resulted in a higher stabilized cloud top altitude and larger volume; Increasing the surface water loading resulted in a lower stabilized cloud top and a smaller cloud volume. The effect of soil loading was also examined, and it was found to produce only slight changes in the stabilized cloud top and volume. The results found with the revised CRM were also compared to the results found using the original CRM. Both versions followed the same trends as the humidity profiles were changed, but the results found

for the surface water loading case were very divergent. The differences in the results of the two versions suggest the results of the revised CRM are more valid.

Introduction

BACKGROUND:

The Defense Land Fallout Information Code, DELFIC, was created in the late 1960's to model nuclear fallout. The code has been revised many times since its creation. The last revision was made during the mid 1970's. DELFIC has served as a standard to judge other codes. The source code is composed of three modules which initialize variables, model the cloud rise, and transport the cloud's particles to the ground. The initial values of the cloud's variables are calculated based on empirical data fits obtained from atmospheric nuclear tests. The cloud rise is modeled as a one-dimensional entrainment bubble based on a set of coupled ordinary differential equations which represent conservation of mass, momentum, heat and turbulent kinetic energy (3:19). The transport model of DELFIC uses a disk tosser approach to distribute the cloud's activity on the ground.

The nuclear fallout cloud modeled by the Cloud Rise Module, CRM, is composed of four elements: surface water, atmospheric water vapor, dry air, and soil. Changing the amount of any of these elements will alter the cloud's final

stabilized height and shape. Nuclear weapon debris is also present in the cloud, but its mass is so small that its presence has little effect on the size and location predicted by the CRM.

The Nuclear Criteria Group at the Air Force Weapons Laboratory recently became interested in how the CRM results are affected by the water content of the cloud. The water in the cloud modeled by the CRM comes from two sources: initial surface water lofted into the fireball, and atmospheric water vapor from air entrained by the cloud. The water in the cloud can affect both the predicted stabilized height and shape of the cloud. Information about how different amounts of water from these two sources affect the results predicted by the CRM was desired by the Nuclear Criteria Group.

PROBLEM:

The purpose of this study was to examine the effect of water content on the predicted height and shape of the cloud modeled by the CRM of DELFIC. During the analysis of the CRM a number of problems were found with it. The purpose was then broadened to include revising the CRM to correct these problems. The effect of water content on the original and

revised CRM predictions were then examined and the results compared.

APPROACH:

The CRM of DELFIC was first examined in detail, and problems were noted. Then the source code of the CRM was examined to confirm that the problems did in fact exist and had not been corrected. All of the problems found with the source code were then corrected and a new version of the CRM was created. The old CRM was compared to the new version on how it handled the cloud's water content from initial surface water and atmospheric water vapor. These results were analyzed and evaluated.

SEQUENCE OF PRESENTATION:

The second chapter covers the basic concepts of the CRM. The third chapter presents the problems found with the CRM and the proposed solutions. The fourth chapter presents the results found on the effect of atmospheric water vapor. The fifth chapter shows the effect of surface water. The sixth chapter shows the effect of changing the initial soil mass for the original CRM. The seventh chapter discusses

some other problems with the CRM. The final chapter presents the conclusions drawn from this study.

A complete list of all the variables used in the equations is presented in the prefatory section. Also a complete list of the changes made to the CRM of DELFIC is given in Appendix A.

The Basics of the Cloud Rise Module

The Cloud Rise Module, CRM, calculations start when pressure equilibrium is reached between the atmosphere and the fireball. The time and temperature were empirically determined as functions of yield and height of burst from atmospheric nuclear testing data (3:9).

During the cloud rise calculation all the soil is assumed to be in a condensed phase. The initial temperature of the condensed soil present is estimated with (3:10):

$$T_{si} = 200*\log_{10}(W) + 1000.0 \qquad (1)$$

where

T_{si} = initial soil temperature of the cloud (K)

W = weapon's yield (Kt)

The initial soil temperature is typically lower than the gas temperature of the cloud. The soil temperature is assumed to stay at its initial value until the cloud's gas temperature reaches equilibrium with it. After reaching equilibrium the condensed soil and cloud gas temperatures are assumed to stay in equilibrium (3:11).

The fraction of the yield initially present in the fireball has been empirically found to be 45 percent of the total yield (3:12). This initial energy present in the fireball is used to determine how much dry air, atmospheric water vapor, and surface water are initially entrained within it. The initial energy present in the fireball is used to heat the soil, dry air, atmospheric water vapor, and surface water. The initial soil mass present in the fireball is determined by an empirical function of both yield and height of burst (3:10). The energy required to heat the initial soil mass in the fireball to its initial temperature is subtracted from the total energy in the fireball to give the energy used to heat the dry air, atmospheric water vapor, and surface water in the fireball. A variable ϕ is defined by DELFIC as the ratio of the energy used to heat dry air and atmospheric water vapor to the energy used to heat surface water, atmospheric water vapor, and dry air. For a given value of ϕ the cloud's initial dry air and water masses are given by (3:12, 13):

$$M_{ai} = \frac{\phi * E_{aw}}{\int_{T_{ei}}^{T_i} C_{pa}(T)dT + x_e \int_{T_{ei}}^{T_i} C_{pw}(T)dT} \qquad (2)$$

$$M_{wi} = \frac{(1 - \phi) * E_{aw}}{\int_{T_{ei}}^{T_i} C_{pw}(T)dT + L} + x_e * M_{ai} \qquad (3)$$

where

$C_{pa}(T)$ = specific heat of dry air (J/(kg*K))

$C_{pw}(T)$ = specific heat of water (J/(kg*K))

E_{aw} = total energy used to heat dry air, atmospheric water vapor, and surface water (J)

$$E_{aw} = 0.45*Y - \int_{T_{ei}}^{T_{si}} C_S(T)dT$$

where: 0.45 = fraction of the yield energy initially in the fireball

Y = weapon's yield energy (J)

L = latent heat of water,vaporization or ice (J/kg)

M_{ai} = initial air mass of the cloud (kg)

M_{wi} = initial water mass of the cloud (kg)

ϕ = ratio of the energy used to heat dry air and atmospheric water vapor to the energy used to heat surface water, atmospheric water vapor, and dry air

$$\phi = E_{a,wv} / (E_{a,wv} + E_{cw})$$

where: $E_{a,wv}$ = energy used to dry air and atmospheric water vapor (J)

E_{cw} = energy used to heat surface

water (J)

T = temperature (K)

T_{ei} = initial ambient temperature at the cloud center altitude (K)

T_i = initial cloud temperature (K)

x_e = atmospheric water vapor mixing ratio at the cloud center altitude = the ratio of the atmospheric water vapor mass to the dry air mass per unit volume

The CRM assumes that no surface water or soil is entrained in the cloud beyond the initial amounts. However, the amounts of dry air and atmospheric water vapor present in the cloud are further increased by the entrainment of the ambient atmospheric air. The amounts of soil and water in the cloud are reduced by fallout of these elements. The distribution of soil, air, and water in the cloud is assumed to be homogeneous at all times.

The cloud's composition and position after the initial time are calculated using a set of coupled ordinary differential equations that represent conservation of mass, momentum, heat and turbulent kinetic energy (3:19). The ambient atmospheric properties used in these equations are taken at the cloud center altitude. The specifics of these

equations will be examined in the next chapter.

The cloud is initially modeled as an oblate spheroid of eccentricity 0.75. This cloud shape is kept constant while its volume changes until the cloud's vertical velocity reaches zero (vertical stabilization), after which the cloud top and base altitudes are held fixed. The radius of the cloud is then allowed to expand until either (1:26-27):

$$\frac{dR_c}{dt} \leq \frac{R_c * W^{0.014778}}{1153.} \tag{4}$$

or

$$E < \max[\ 10,\ \min(\ 23 + 9*\log(W),\ 60\ )\ ] \tag{5}$$

where

E = turbulent kinetic energy density per unit mass (J)

R_c = horizontal cloud radius (m)

Once one of these criteria is met, the cloud has also achieved horizontal stabilization and the CRM calculations are stopped. Equation (4) is one of several purely empirical relations in the present CRM of DELFIC.

The cloud volume is calculated using the ideal gas

equation (3:26):

$$V = (R_a * T_v * M_g) / P \qquad (6)$$

where

M_g = mass of the gases contained in the cloud, dry air and atmospheric water vapor (kg)

P = pressure (Pa)

R_a = ideal gas constant = 287. (J/(kg*K))

T_v = cloud virtual temperature (K)

$$T_v = T*(1 + x/\epsilon)/(1 + x)$$

V = cloud volume (m^3)

x = water vapor mixing ratio in the cloud

ϵ = ratio of molecular weights of water and air

$$\epsilon = (18.0 / 29.0)$$

The virtual temperature is an artificial temperature used to take into account that the cloud is composed of both gases and condensed matter.

The Problems with the CRM

The cloud rise module models the nuclear cloud as a dynamic, one-dimensional, entrainment bubble. The basis of this model is a set of coupled ordinary differential equation which represent conservation of mass, momentum, heat, and turbulent kinetic energy (3:19). The properties of the cloud at its center are used in these differential equations as if they applied globally. The differential equations in DELFIC are solved using a fourth-order Runge-Kutta algorithm.

The modeling of the CRM presented in its documentation was first examined and potential problems noted. Then the source code of the CRM was examined to confirm that these errors were present. Other problems with the source code were also found during this examination. The errors in the CRM come from two different sources: mistakes in the physics of the model, and mistakes in the source code. The problems with the physics of the CRM are the result of theoretical inconsistencies, while the errors in the source code are apparently programming errors.

Because the derivations of the differential equations used by the CRM are so lengthy, only a synopsis of the equations, problems found, and solutions proposed are presented here. The thorough presentation of the

derivations of the differential equations can be found in the referenced sources.

The differential equation for momentum used by the CRM is (3:19):

$$(du/dt) = \overset{(a)}{\left(\frac{T_v}{T_{ev}}\beta' - 1\right)} g - \left[\overset{(b)}{\left(\frac{2*K_2*v*T_v*(1+x)}{H_c*T_{ev}*(1+x+w+s)} \right)} + \overset{(c)}{(1/M)*(dM/dt)_{ent}} \right] u \qquad (7)$$

where

g = acceleration due to gravity (m/sec)

$g = 9.8$ (m/sec)

H_c = vertical radius of the cloud (m)

K_2 = dimensionless empirical parameter, used in the eddy viscosity term

M = mass of the cloud (kg)

$(dM/dt)_{ent}$ = change of the entrained cloud mass with respect to time (kg/sec)

s = soil mixing ratio = the ratio of the mass of soil to the unit mass of dry air containing it.

T_{ev} = ambient virtual temperature (K)

$$T_{ev} = T_e*(1 + x_e/\epsilon)/(1 + x_e)$$

u = cloud vertical velocity (m/sec)

v = cloud's characteristic velocity (m/sec)

$$v = \max[\ |u|,\ (2*E)^{\wedge}0.5\ ]$$

w = water mixing ratio = the ratio of the mass of water to the unit mass of dry air containing it.

β' = ratio of the cloud's atmospheric water vapor and dry air density to its total density

$$\beta' = (1 + x)/(1 + x + w + s)$$

The terms (a), (b), and (c) represent respectively the forces of buoyancy, eddy-viscous drag, and entrainment drag (3:20). This equation is correct, but an error in the source code caused it to be incorrectly implemented. The term (b) in the equation is incorrectly represented in the source code as:

$$\left(\frac{2*K_2*v*T_v*(1+x+w)}{H_c*T_{ev}*(1+x+w+s)}\right) \tag{8}$$

This error in the source code was corrected.

The differential equation for turbulent kinetic energy per unit mass used in the CRM is (3:12):

$$(dE/dt) = \overset{(a)}{\left(\frac{2*K_2*T_v*(u^{\wedge}2)*v*(1+x)}{T_{ev}*H_c*(1+x+w+s)}\right)} + \overset{(b)}{\left(\frac{u^{\wedge}2}{2*M}\right)*(dM/dt)_{ent}}$$

$$- \overset{(c)}{(E/M)*(dM/dt)_{ent}} - \overset{(d)}{\left(\frac{K_3*(2*E)^{\wedge}1.5}{H_c}\right)} \tag{9}$$

where

K_3 = dimensionless empirical parameter, used in the energy dissipation term

The term (a) represents the turbulent kinetic energy per unit mass, E, generated by eddy-viscous drag. Term (b) represents the amount of E generated by momentum-conserving inelastic-collision entrainment. Term (c) represents the dilution of E by the entrainment of air and term (d) represents the dissipation of E to heat (5:12). This equation is correct, however term (a) is incorrectly represented in the source code as:

$$\left(\frac{2*K_2*T_v*(u\hat{\ }2)*v*(1+x+w)}{T_{ev}*H_c*(1+x+w+s)} \right) \qquad (10)$$

This error in the source code was corrected.

Since the entrainment is assumed to be a constant pressure process, an enthalpy balance technique can be used to obtain the differential equation for the cloud's temperature (5:5). For the dry case, when the cloud contains no condensed water, the differential equation for temperature was found to be:

$$(dT/dt) = -(\beta'/C_{pv})\left[\int_{T_e}^{T} C_p(T)dT * \overset{(a)}{\left(\frac{(dM/dt)_{ent}}{\beta' * M}\right)} + \overset{(b)}{(T_v/T_{ev})*g*u} - \overset{(c)}{\varepsilon}\right] \quad (11)$$

where

$C_p(T)$ = weighted specific heat of dry air and atmospheric water vapor (J/(kg*K))

$$C_p(T) = (C_{pa}(T) + x*C_{pw}(T))/(1.0 + x)$$

$C_{pv}(T)$ = weighted specific heat of the cloud for the dry case (J/(kg*K))

$$C_{pv}(T) = \beta' * C_p(T) + (1-\beta')*C_s(T)*k(T,T_{si})$$

where: $k(T,T_{si}) = 1$ if $T_{si} >= T$

$k(T,T_{si}) = 0$ if $T_{si} < T$

T_e = ambient temperature at the cloud center altitude (K)

ε = energy dissipation rate (J/(kg*sec))

This was obtained by following the derivation presented in the documentation (5:5-8). The only change was that the air entrained by the cloud was assumed to contain both dry air and atmospheric water vapor. However, the result presented in the CRM documentation and in the source code (5:8) assumed that only dry air was entrained by the cloud for the

dry case. The resulting difference between these two treatments is that in the documented version (5:8) the equation for term (a) is:

$$\int_{T_e}^{T} C_{pa}(T)dT * \left(\frac{(dM/dt)_{ent}}{\beta' * M} \right) \qquad (12)$$

The entrained air in the cloud must be composed of both dry air and atmospheric water vapor. Therefore, equation (11) replaced the documented equation in the source code.

For the wet case, when the cloud contains condensed water, the differential equation for temperature is (5:10):

$$(dT/dt) = -\frac{\beta'}{[1 + (L^{\wedge}2)*x*\epsilon/(C_p*R_a*(T^{\wedge}2))]} \left[\left\{ (T-T_e) + \frac{L*(x-x_e)}{C_p} \right\} \left(\frac{(dM/dt)_{ent}}{M * \beta'} \right) - (\epsilon/C_p) + \left(\frac{T_v*g*u}{T_{ev}*C_p} \right) \left[1 + \frac{L*x}{R_a*T} \right] \right] \qquad (13)$$

This equation is correct, and there were no problems found with the source code representing it.

The differential equation describing the rate of change of the mass entrained by the cloud is obtained by

differentiating the ideal gas equation and expressing it in terms of known cloud quantities. The resulting equation for the dry case is (5:34):

$$(dM/dt)_{ent} = \frac{\dot{M} * \beta'}{\left[1 - \underbrace{\left(\frac{\beta'}{C_{pv} * T_v}\right)}_{(a)} \underbrace{\left(\int_{T_e}^{T} C_p(T)dT\right)}_{(b)} \right]} \left\{ \frac{\dot{\mu} * v * S}{V} + \left(\frac{\beta'}{C_{pv} * T_v}\right)\left[\left(\frac{T_v}{T_{ev}}\right) * g * u - \mathcal{E}\right] - \left(\frac{g * u}{R_a * T_e}\right)\right\} \quad (14)$$

The only difference between this result and the equation presented in the documentation (5:13) is the term (b) in the current code is given by:

$$\int_{T_e}^{T} C_{pa}(T)dT \quad (15)$$

This result is obtained because again the documented derivation assumes the cloud only entrains dry air. The assumption is incorrect because the air entrained by the cloud must be composed of both dry air and atmospheric water vapor. Therefore equation (14) was used in place of its documented counter part for this case. The source code also

had term (a) incorrectly represented as:

$$\left(\frac{1}{Cp*T}\right) \qquad (16)$$

This is an apparent programming error and it was corrected to make the source code consistent with equation (14).

The differential equation for the rate of change of mass entrained by the cloud for the wet case is (5:14):

$$(dM/dt)_{ent} = \frac{M * \beta'}{\left\{1 - \left(\frac{\beta'}{T_v}\right)\left[\frac{1}{1 + \frac{(L\hat{}2)*x*\epsilon}{C_p*R_a*(T\hat{}2)}}\right]\left[\left(T-T_e\right) + \frac{L*(x-x_e)}{C_p}\right]\right\}}$$

$$* \left\{\frac{\mu*v*S}{V} + \left(\frac{\beta'}{T_v}\right)\left[\frac{1}{1 + \frac{(L\hat{}2)*x*\epsilon}{C_p*R_a*(T\hat{}2)}}\right]\right.$$

$$\left. * \left[\left(\frac{T_v*g*u}{T_{ev}*C_p}\right)\left(1 + \frac{L*x}{R_a*T}\right) - \frac{\epsilon}{C_p}\right] - \left(\frac{g*u}{R_a*T_{ev}}\right)\right\} \qquad (17)$$

where

μ = dimensionless empirical constant used in entrainment equation

This equation is correct, and no problems were found with

the source code.

The differential equation describing how the cloud's mass changes with time for the dry case is :

$$(dM/dt) = (dM/dt)_{ent} - P_S(t) \qquad (18)$$

where

$$P_S(t) = PI*(R_c\hat{}2)*\rho_{PS} *\sum_j f_j * [(PI/6)*(D_{sj}\hat{}3)] *n_s(t)_j \qquad (19)$$

where

D_{sj} = mean soil particle diameter in the jth group (m)

f_j = terminal velocity of a particle in the jth size group (m/sec)

$n_S(t)_j$ = the number of soil particles in the jth group per unit volume of the cloud (1/m^3)

ρ_{PS} = density of a soil particle (kg/m^3)

$P_S(t)$ = soil mass fallout rate from the cloud (kg/sec)

This equation is correct since only soil is lost from the cloud for the dry case. No problems were found in the source code.

The documented differential equation describing the cloud's rate of change of mass for the wet case is also given by equation (18). It contains no term to take into

account the water loss rate from the cloud (5:14). The actual differential equation for the wet case must be:

$$(dM/dt) = (dM/dt)_{ent} - P_s(t) - P_w(t) \tag{20}$$

where

$$P_w(t) = PI*(R_c\hat{\ }2)*\rho_{pw}*\sum_j f_j * [(PI/6)*(D_{wj}\hat{\ }3)] *n_w(t)_j \tag{21}$$

where

D_{wj} = mean water particle diameter in the jth group (m)

$n_w(t)_j$ = the number of water particles in the jth group per unit volume of the cloud (1/m^3)

$P_w(t)$ = water mass fallout rate from the cloud (kg/sec)

ρ_{pw} = density of a water particle (kg/m^3)

Where the function $P_s(t)$ is a new addition to the code to take into account the mass loss rate of water from the cloud. A very simple model of water rainout was used which assumed that all droplets were the same size with a diameter of 0.1 mm (2:314). This simple model allows the cloud's rate of mass change to be modeled for the wet case. The examination of the cloud's source code for these equations found the terminal settling speed equation for particles in still air to completely contradict the documented equation for Davies numbers, N_d, greater than 140 and less than

4.5x10^7 (3:25)(1:259). The correct equation for the terminal settling speed of particles for this case is:

$$f = \left(\frac{\eta}{\rho * D_p} \right) * 10.^{Z} \qquad (22)$$

where

$$Z = [-1.29536 + 0.986*X - 0.046677*(X\hat{}2) + 0.0011235*(X\hat{}3)] \qquad (23)$$

$$X = \log(N_d) \qquad (24)$$

$$N_d = \left(\frac{4* \rho *(\rho_p - \rho)*g*(D_p\hat{}3)}{3*(\eta \hat{}2)} \right) \qquad (25)$$

D_p = diameter of particle (m)

N_d = Davies number

η = dynamic viscosity of the cloud gas (kg/(m*sec))

ρ = density of the cloud (kg/m^3)

ρ_p = density of a particle (kg/m^3)

This error was corrected in the source code. Also the criteria of N_d = 140 as the dividing point between the two equations for f was changed to N_d = 100. This was changed because it produces a smoother transition between the two fits for f.

The water vapor mixing ratio in the cloud is described by two different equations, one for the dry case and one for the wet case. The differential equation for the dry case is (5:5):

$$(dx/dt) = -\left(\frac{(1+x+s)*(x-x_e)}{M * (1 + x_e)}\right) * (dM/dt)_{ent} \qquad (26)$$

The differential equation for the wet case is (5:5):

$$(dx/dt) = x*(1 + x/\epsilon)\left[\left(\frac{L*\epsilon}{R_a*(T\hat{}2)}\right) *(dT/dt) + \left(\frac{g*u}{R_a*T_{ev}}\right)\right] \qquad (27)$$

Both of these equations are correct, and no problems were found with their representation in the source code.

The differential equation describing the cloud's soil mixing ratio was found to be:

$$(ds/dt) = -\frac{(1+x+w+s)}{m}\left[\left(\frac{s}{1 + x_e}\right) *(dM/dt)_{ent} + \overset{(a)}{P_s(t)}\right] \qquad (28)$$

The difference between this equation and the documented equation (5:15) is that term (a) in equation (28) is represented as:

$$\left(\frac{s}{s + w}\right) * P(t) \qquad (29)$$

where

$P(t)$ = total mass fallout rate from the cloud (kg/sec)

The reason for this difference is that the documentation claimed $P(t)$ was the total fallout rate from the cloud, and multiplying it by $[s/(w + s)]$ would result in the soil fallout rate. This is not correct because $P(t)$ in the documentation (5:14) is not the total fallout rate, it is the soil fallout rate. If $P(t)$ was the total fallout rate from the cloud the soil fallout rate would be given by:

$$P_S(t) = P(t) - P_W(t) \qquad (30)$$

Since the value of $P(t)$ used by the source code of the CRM is actually $P_S(t)$, the fraction $[s/(w + s)]$ was dropped from the source code equation.

The differential equation describing the cloud's water mixing ratio was found to be:

$$(dw/dt) = -\frac{(1+x+w+s)}{M}\left[\frac{(w + x - x_e)}{(1 + x_e)} * (dM/dt)_{ent} - P_w(t)\right] - (dx/dt) \qquad (31)$$

The documentation (5:11) claims the value of $P_W(t)$ is:

$$P_W(t) = \left(\frac{w}{(s + w)}\right) * P(t) \qquad (32)$$

Since the value of P(t) used by the source code is actually the soil fallout rate, $P_S(t)$, this is not correct. But regardless of whether P(t) is the total fallout rate from the cloud, or the soil fallout rate, equation (32) is incorrect. The correct equation for the water fallout rate is equation (21), and this correction was made to the water mixing ratio differential equation.

The revisions described above changed how the CRM calculates water and soil fallout, and the composition of the entrained air for the dry case.

The Effect of Atmospheric Water Vapor on the CRM

The original and revised versions of the CRM were examined to see how atmospheric water vapor affects cloud height and volume. The results of the two versions of the CRM were then compared. Three different atmospheric profiles were used to study the effect of atmospheric humidity on these versions of the CRM. These profiles contain atmospheric data such as temperature, air density, pressure, relative humidity, and viscosity at incremented altitudes. The atmospheric profile specified by the user is then used by the CRM in its calculations. The first atmospheric profile used was the U.S. Standard Atmosphere Mid Latitude Spring / Fall, MIDLSF, which is an averaged middle latitude spring-fall profile. The second atmospheric profile used was the MIDLSF profile with no relative humidity present at any altitude. This profile was referred to as the 0.0 Humidity profile. The last profile used was the Handbook of Geophysics (1965) Modified Tropic Atmosphere, TROPIC, which represents a tropical atmosphere with a high relative humidity content. These humidity profiles were used for runs of each version of the CRM for the following yields: 1kt, 10kt, 100kt, 1Mt, 5Mt, 10Mt, 15Mt, 20Mt.

The results for only the revised CRM will be shown in this section. The results found using the original CRM for these same cases and the comparison of the results found with both versions of the CRM are shown in Appendix C. All of these results will be discussed and a possible explanation posed.

The stabilized top altitude and cloud volume for the MIDLSF and TROPIC profile results were compared to the result of the 0.0 Humidity Profile. These results for the revised CRM are shown in Tables I and II. Graphically, the stabilized cloud top data is shown in Figure 1, and a comparison of the results for the MIDLSF and TROPIC profiles verses the 0.0 Humidity profile is presented in Figure 2. The predicted volume of the stabilized cloud by the revised CRM is shown Figure 3, and the change in the results found with the MIDLSF and TROPIC profiles compared to the 0.0 Humidity Profile result is shown in Figure 4.

The changes in stabilized top altitude and volume of the cloud are found to follow the same general trends as the yield is changed for both versions of the CRM. For most yields the cloud stabilized top altitude was highest for the TROPIC profile, and lowest for the 0.0 humidity profile for either version of the CRM. Also, the largest stabilized cloud volume was generally found to be for the TROPIC

profile, and the smallest for the 0.0 Humidity profile, regardless of the version.

For humid atmospheres the cloud will entrain large amounts of atmospheric water vapor. When the temperature and pressure become correct in the cloud the water vapor it contains will condense and rainout of the cloud, releasing its latent heat of vaporization energy. This added energy to the cloud rise results in the cloud taking longer to reach stabilization. Therefore, the resulting stabilized cloud will have a higher top altitude and larger volume, because it will have a longer period to rise and entrain air. It is expected then that a more humid atmosphere will cause the stabilized cloud to have a higher top altitude and larger volume. This exact trend is observed for both versions of the DELFIC CRM.

The values of the stabilized top altitude and cloud volume for each of the three humidity profiles for the original CRM was compared to the results from the revised CRM. The stabilized top altitude of the cloud was comparable for all three humidity profiles of both versions for yields from 1kt to 1Mt, and was higher for the new version of CRM for yields larger than 1Mt. The original CRM predicted a larger stabilized cloud volume for the lower yields than the revised version for all three humidity

profiles. For yields larger than 10Mt the situation is reversed and the original CRM predicts a smaller stabilized cloud volume than the revised version for all three atmospheric profiles.

Table I. Comparing Stabilized Cloud Top of the MIDLSF and TROPIC Profile Results to the 0.0 Humidity Profile Result - Revised CRM

Yield (Kt)	Humidity Profile	Profile Cloud Top (m)	0.0 Humidity Cloud Top (m)	Percent Change in Cloud Top
1.0	MIDLSF	3182.	3086.	3.1
1.0	TROPIC	2743.	3086.	-11.1
10.0	MIDLSF	6628.	6297.	5.3
10.0	TROPIC	5986.	6297.	-4.9
100.0	MIDLSF	11980.	11230.	6.7
100.0	TROPIC	13980.	11230.	24.5
1000.0	MIDLSF	18280.	18020.	1.4
1000.0	TROPIC	22310.	18020.	23.8
5000.0	MIDLSF	26500.	26300.	0.7
5000.0	TROPIC	29370.	26300.	11.7
10000.0	MIDLSF	33560.	33360.	0.6
10000.0	TROPIC	35560.	33360.	6.6
15000.0	MIDLSF	40100.	39870.	0.6
15000.0	TROPIC	41840.	39870.	4.9
20000.0	MIDLSF	46650.	46380.	0.6
20000.0	TROPIC	47970.	46380.	3.4

Table II. Comparing Stabilized Cloud Volume of the MIDLSF and TROPIC Profile Results to the 0.0 Humidity Profile Result - Revised CRM

Yield (Kt)	Humidity Profile	Profile Cloud Volume (m^3)	0.0 Humidity Cloud Volume (m^3)	Percent Change in Cloud Volume
1.0	MIDLSF	1.883E9	1.820E9	3.5
1.0	TROPIC	1.147E9	1.820E9	-37.0
10.0	MIDLSF	1.246E10	1.238E10	0.6
10.0	TROPIC	1.029E10	1.238E10	-16.9
100.0	MIDLSF	2.465E11	2.211E11	11.5
100.0	TROPIC	2.626E11	2.211E11	18.8
1000.0	MIDLSF	4.085E12	3.927E12	4.0
1000.0	TROPIC	5.503E12	3.927E12	40.1
5000.0	MIDLSF	2.335E13	2.612E13	-10.6
5000.0	TROPIC	3.142E13	2.612E13	20.3
10000.0	MIDLSF	6.604E13	6.608E13	-0.06
10000.0	TROPIC	7.452E13	6.608E13	12.8
15000.0	MIDLSF	1.274E14	1.274E14	0.0
15000.0	TROPIC	1.385E14	1.274E14	8.7
20000.0	MIDLSF	2.209E14	2.196E14	0.6
20000.0	TROPIC	2.252E14	2.196E14	2.6

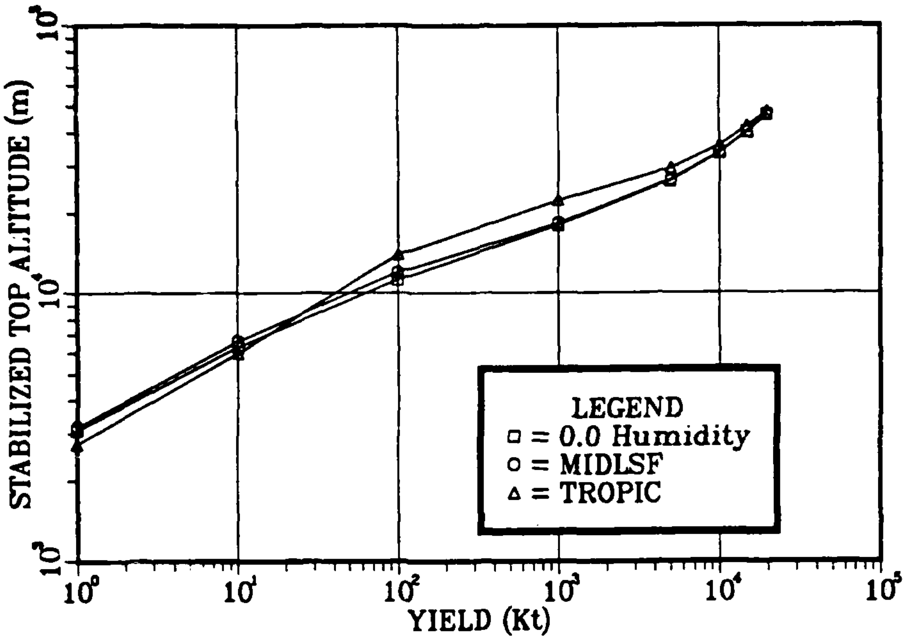

Figure 1. The Effect of Atmospheric Water Vapor on the Stabilized Cloud Top Altitude - Revised CRM

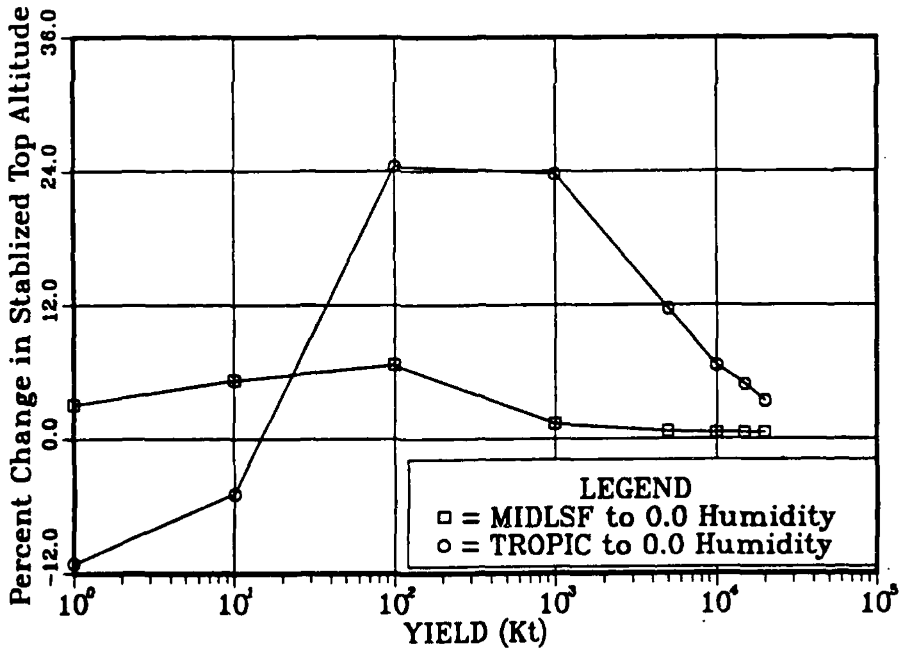

Figure 2. Comparing Stabilized Cloud Top of the MIDLSF and TROPIC Profile Results to the 0.0 Humidity Profile Result - Revised CRM

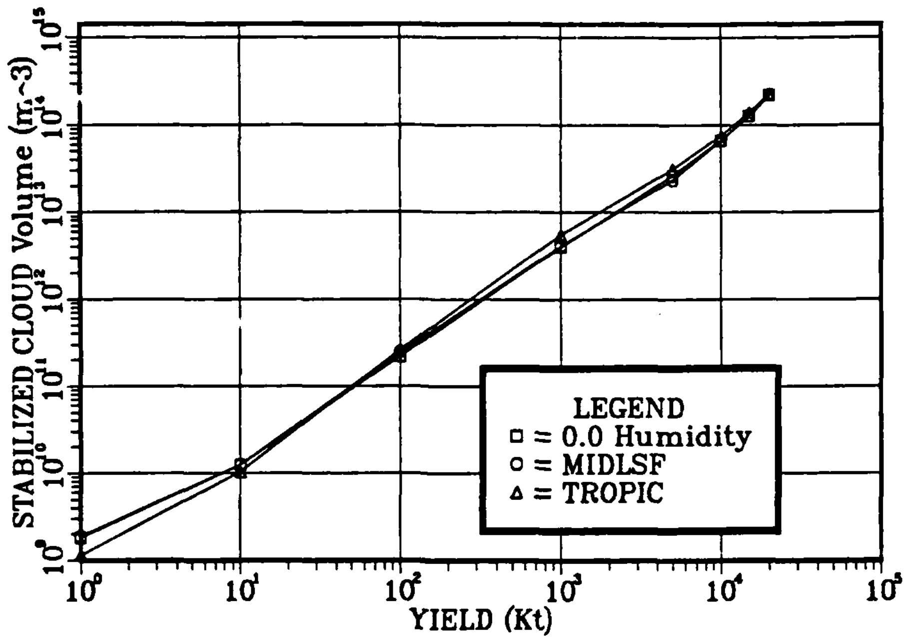

Figure 3. The Effect of Atmospheric Water Vapor on the Stabilized Cloud Volume - Revised CRM

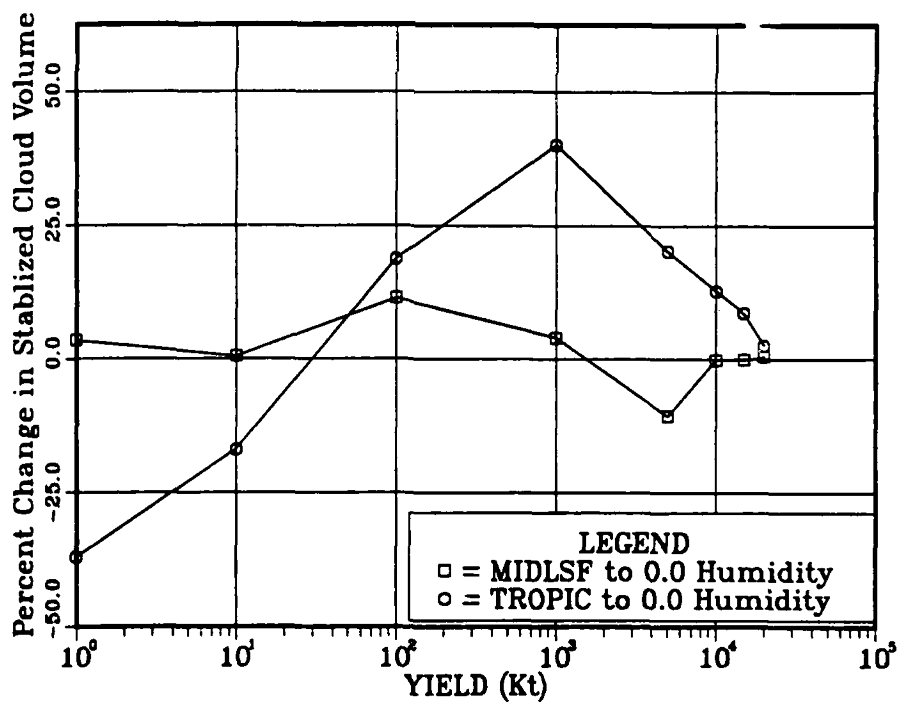

Figure 4. Comparing Stabilized Cloud Volume of the MIDLSF and TROPIC Profile Results to the 0.0 Humidity Profile Result - Revised CRM

The Effect of Surface Water on the CRM

The effect of changing the cloud surface water mass was examined for each version of the CRM. The value of ϕ was varied to change the amount of initial water mass in the cloud. The smaller the value of ϕ, the more initial water mass present in the cloud. The 0.0 Humidity profile was used for all the cases examined, so all the water present in the cloud was from the surface water mass. Three values of ϕ were used: 1.0, 0.5, and 0.1. These values of ϕ were used for each of the following yields: 1kt, 10kt, 100kt, 1Mt, 5Mt, 10Mt, 15Mt, and 20Mt.

The amount of water present in the initial cloud for a given value of ϕ is a hard value to visualize. To give insight into this relationship a computer program was created to calculate the initial amount of water, dry air, and soil present in the cloud for a given value of ϕ, yield, and set of atmospheric conditions. It uses the exact same equations used by the CRM to calculate these initial values. The results for the yields and ϕ values used in this study with 0.0 relative humidity, an ambient temperature of 295 K, and atmospheric pressure of 1.0 atmosphere are shown in Table III. The source code of the C

program used to calculate these values is shown in Appendix B.

The results for only the revised CRM will be shown in this section. The results found using the original CRM and the comparison of the predictions of both versions of the CRM are presented in Appendix D. All of these results are discussed in this section, and appropriate conclusions drawn.

The stabilized top altitude and cloud volume for ϕ = 0.5 and ϕ = 0.1 were first compared to values found with ϕ = 1.0 . The results found with the revised CRM are shown in Tables IV and V. The predicted stabilized cloud top altitude is shown in Figure 5, and the cloud volume is shown in Figure 7. The change in the cloud's stabilized top altitude for ϕ = 0.5 and ϕ = 0.1 compared to ϕ = 1.0 is shown graphically in Figure 6, and the change in the stabilized cloud volume in Figure 8.

For the revised version of the CRM, the ϕ = 1.0 case had the highest stabilized top altitude for each yield, ϕ = 0.5 had the intermediate altitude, and ϕ = 0.1 was the lowest case. The exact opposite was true for the original CRM. As more surface water is added to the initial cloud the less dry air and water vapor it can contain. Therefore, as ϕ is decreased in value the density of the

initial cloud is increased. The resulting effect of this increased density should be a lowered stabilized cloud top altitude, because more energy will be required to lift the denser cloud to a given altitude. Therefore, the altitude of the stabilized cloud top should become lower as the value of ϕ is decreased. The only version that obeys this prediction is the revised CRM, therefore it is more valid for this case.

The volume of the stabilized cloud became smaller as ϕ became smaller for yields less than 1 Mt for both CRM versions, but the reduction in cloud volume with ϕ was much more rapid for the revised version. For yields greater than 1 Mt, the revised CRM continued to follow this same trend. The original CRM did just the opposite, predicting for the higher yields that the cloud volume would become larger as ϕ became smaller. As ϕ becomes smaller the amount of water present in the initial cloud increases and composes a larger portion of the cloud's volume. The majority of the water present in the cloud will condense and fallout of the cloud long before it reaches its stabilized volume. Therefore, the volume of a cloud initially containing more water than another one , for a given yield, will have a smaller final stabilized cloud volume. So as the value of ϕ is decreased it is expected that the volume

of the final stabilized cloud should also decrease. This predicted behavior was followed by both versions of the CRM for yields less than 1 Mt, but only by the revised version for yields greater than 1 Mt.

The values produced by each of the CRM versions were compared for each yield and each value of ϕ . The original CRM stabilized top altitude for $\phi = 1.0$ was shorter than the revised CRM for all the yields examined; while the opposite was found for $\phi = 0.5$ and $\phi = 0.1$. For $\phi = 1.0$ with yields 1kt to 100kt, the revised CRM predicted a smaller stabilized cloud volume than the original CRM, but for the higher yields, the revised version cloud volume was larger than the original. For $\phi = 0.5$ and $\phi = 0.1$, the revised CRM predicted a smaller stabilized cloud volume than the original CRM for all the yields examined.

Table III. Initial Masses of Soil, Dry Air, and Water Present in the Cloud

Atmospheric Conditions: Temperature = 295°K
Pressure = 1.0 atm
Relative Humidity = 0.0

Yield (Kt)	ϕ	Mass Soil (kg)	Mass Air (kg)	Mass Water (kg)	Mass Cloud (kg)	Volume Cloud (m^3)
1.0	1.0	9.03e5	4.51e5	0.0	1.35e6	3.18e6
1.0	0.5	9.03e5	2.25e5	6.25e4	1.19e6	1.86e6
1.0	0.1	9.03e5	4.51e4	1.13e5	1.06e6	8.09e5
10.0	1.0	6.89e6	4.33e6	0.0	1.12e7	3.13e7
10.0	0.5	6.89e6	2.17e6	6.07e5	9.66e6	1.84e7
10.0	0.1	6.89e6	4.33e5	1.09e6	8.41e6	8.02e6
100.0	1.0	5.25e7	4.10e7	0.0	9.35e7	3.10e8
100.0	0.5	5.25e7	2.05e7	5.90e6	7.89e7	1.83e8
100.0	0.1	5.25e7	4.10e6	1.06e7	6.72e7	8.09e7
1000.0	1.0	4.01e8	3.65e8	0.0	7.66e8	3.00e9
1000.0	0.5	4.01e8	1.83e8	5.58e7	6.39e8	1.78e9
1000.0	0.1	4.01e8	3.65e7	1.00e8	5.38e8	8.11e8
5000.0	1.0	1.66e9	1.57e9	0.0	3.23e9	1.40e10
5000.0	0.5	1.66e9	7.87e8	2.60e8	2.70e9	8.45e9
5000.0	0.1	1.66e9	1.57e8	4.67e8	2.28e9	3.99e9
10000.0	1.0	3.06e9	2.88e9	0.0	5.94e9	2.68e10
10000.0	0.5	3.06e9	1.44e9	4.97e8	4.99e9	1.63e10
10000.0	0.1	3.06e9	2.88e8	8.95e8	4.24e9	7.86e9
15000.0	1.0	4.37e9	4.07e9	0.0	8.44e9	3.90e10
15000.0	0.5	4.37e9	2.04e9	7.24e8	7.13e9	2.38e10
15000.0	0.1	4.37e9	4.07e8	1.30e9	6.08e9	1.17e10
20000.0	1.0	5.63e9	5.19e9	0.0	1.08e10	5.08e10
20000.0	0.5	5.63e9	2.60e9	9.44e8	9.17e9	3.11e10
20000.0	0.1	5.63e9	5.19e9	1.70e9	7.85e9	1.54e10

Table IV. Comparing Stabilized Cloud Top for ϕ = 0.5 and ϕ = 0.1 to the ϕ = 1.0 Result - Revised CRM

Yield (Kt)	ϕ	ϕ Cloud Top (m)	ϕ = 1.0 Cloud Top (m)	Percent Change in Cloud Top
1.0	0.5	2899.	3086.	-6.1
1.0	0.1	2730.	3086.	-11.5
10.0	0.5	5954.	6297.	-5.4
10.0	0.1	5642.	6297.	-10.4
100.0	0.5	10620.	11230.	-5.4
100.0	0.1	10080.	11230.	-10.2
1000.0	0.5	17480.	18020.	-3.0
1000.0	0.1	17120.	18020.	-5.0
5000.0	0.5	25200.	26300.	-4.2
5000.0	0.1	24580.	26300.	-6.5
10000.0	0.5	31720.	33360.	-4.9
10000.0	0.1	30690.	33360.	-8.0
15000.0	0.5	37860.	39870.	-5.0
15000.0	0.1	36510.	39870.	-8.4
20000.0	0.5	43670.	46380.	-5.8
20000.0	0.1	42000.	46380.	-9.4

Table V. Comparing Stabilized Cloud volume for Φ = 0.5 and Φ = 0.1 to the Φ = 1.0 Result - Revised CRM

Yield (Kt)	Φ	Φ Cloud Volume (m^3)	Φ = 1.0 Cloud Volume (m^3)	Percent Change in Cloud Volume
1.0	0.5	1.389E9	1.820E9	-23.7
1.0	0.1	1.037E9	1.820E9	-43.0
10.0	0.5	8.923E9	1.238E10	-27.9
10.0	0.1	6.958E9	1.238E10	-43.8
100.0	0.5	1.605E11	2.211E11	-27.4
100.0	0.1	1.047E11	2.211E11	-52.6
1000.0	0.5	3.079E12	3.927E12	-21.6
1000.0	0.1	2.216E12	3.927E12	-43.6
5000.0	0.5	2.109E13	2.612E13	-19.3
5000.0	0.1	1.739E13	2.612E13	-33.4
10000.0	0.5	5.081E13	6.608E13	-23.1
10000.0	0.1	3.990E13	6.608E13	-39.6
15000.0	0.5	9.536E13	1.274E14	-25.1
15000.0	0.1	7.436E13	1.274E14	-41.6
20000.0	0.5	1.589E14	2.196E14	-27.6
20000.0	0.1	1.216E14	2.196E14	-44.6

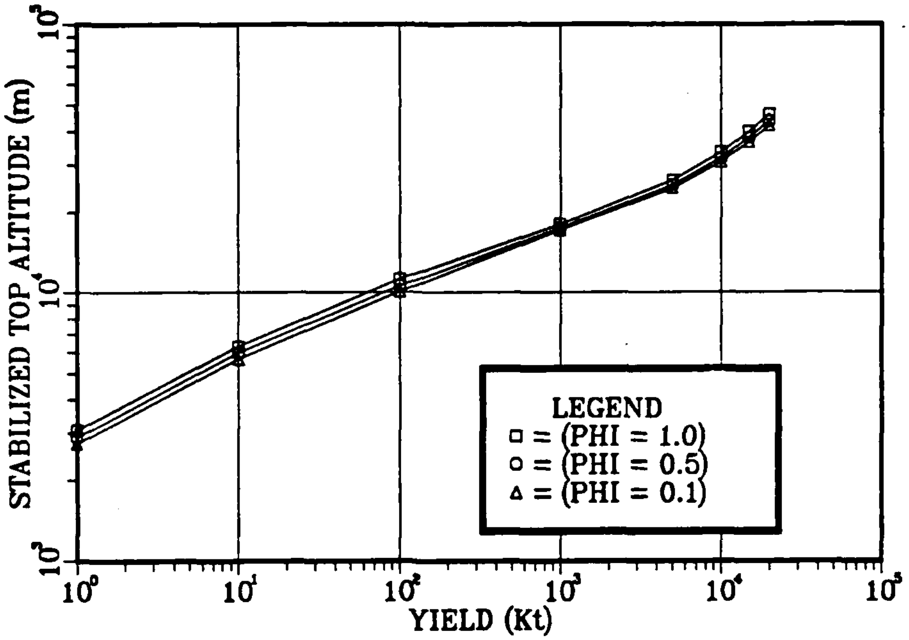

Figure 5. The Effect of Surface Water on the Stabilized Cloud Top Altitude - Revised CRM

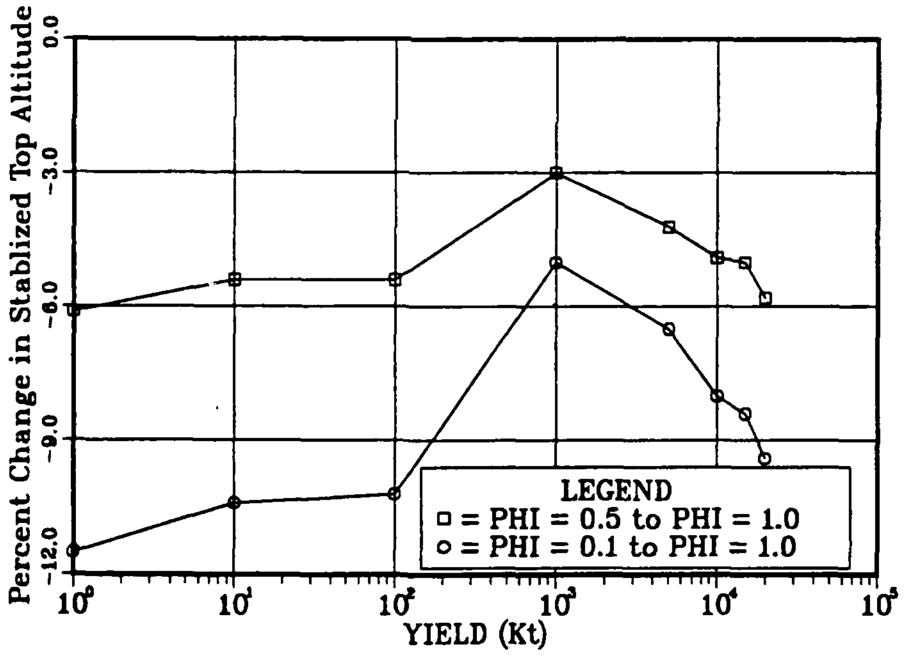

Figure 6. Comparing Stabilized Cloud Top for ϕ = 0.5 and ϕ = 0.1 to the ϕ = 1.0 Result - Revised CRM

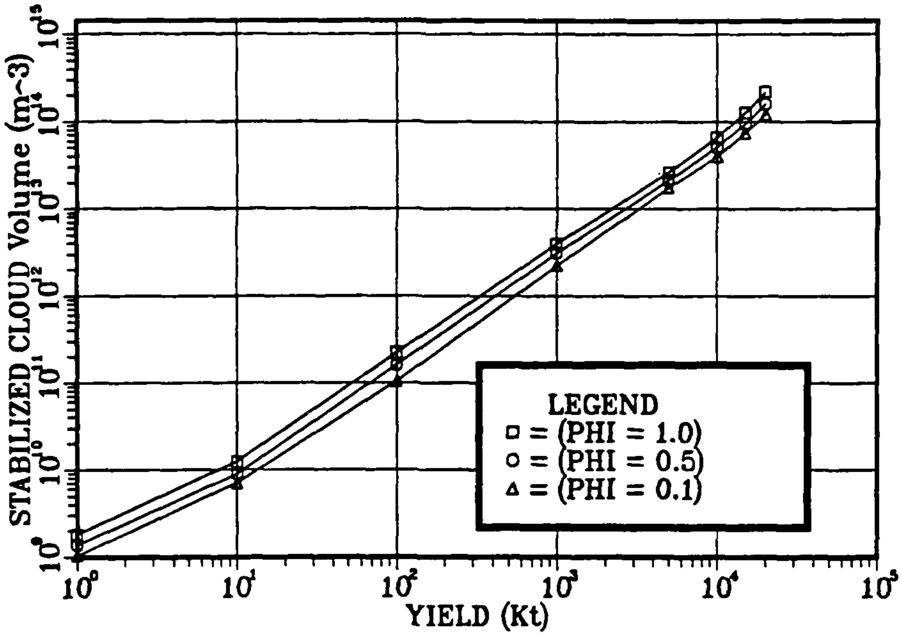

Figure 7. The Effect of Surface Water on the Stabilized Cloud Volume - Revised CRM

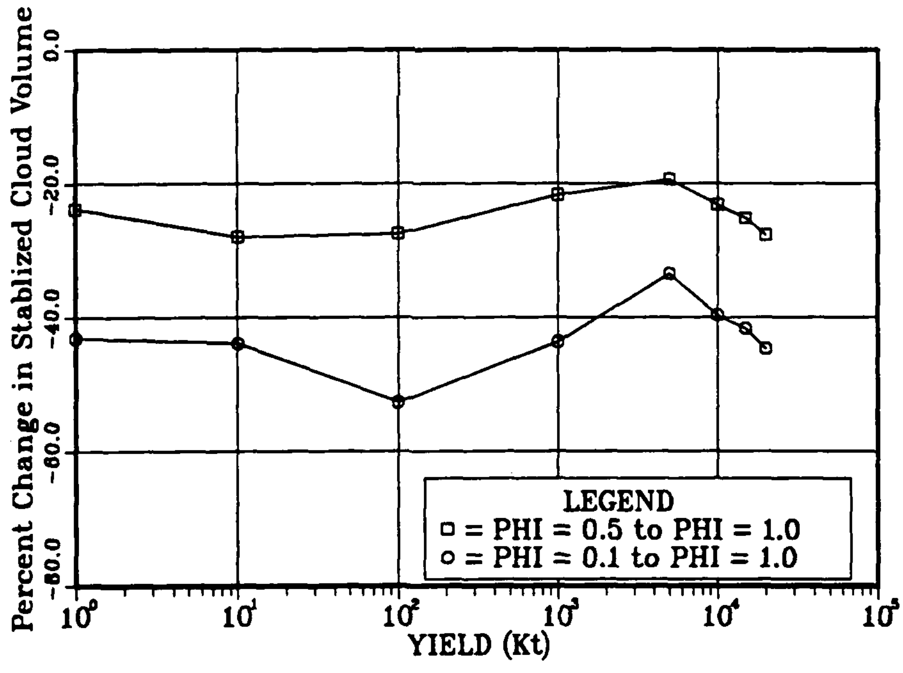

Figure 8. Comparing Stabilized Cloud Volume for ϕ = 0.5 and ϕ = 0.1 to the ϕ = 1.0 Result - Revised CRM

Changing the Initial Soil Mass

The amount of soil present in the cloud for subsurface bursts is based on Nordyke's scaling function for high explosive cratering results (3:10). For surface and above surface bursts the amount of soil in the cloud is calculated based on an empirical relationship between the intersection of the fireball with the ground and the initial soil mass present in the fireball (3:10). The effect of changing the initial soil mass in the cloud predicted by the original CRM was examined for surface burst weapons of yields: 1Kt, 10Kt, 100Kt, 1Mt, 10Mt, and 20Mt. The amount of soil in the initial fireball of the CRM was set at its normal initial amount, twice this amount, and then half this amount. A value of = 1.0 and the MIDLSF humidity profile was used for all the cases examined. This study was not repeated in detail for the revised CRM, because the revisions made in the CRM did not significantly change the way it handles its initial soil mass.

The stabilized cloud top altitude data is shown in Table VI, a graph of the actual data is presented in Figure 9, and a comparison of the results are shown graphically in Figure 10. The stabilized cloud volume data is shown in Table VII, a graph of the results are shown in Figure 11,

and a comparison of the results are shown graphically in Figure 12. For all but the 20Mt case, the smaller the amount of soil present in the initial fireball the higher the stabilized top altitude and the larger the stabilized cloud volume. These results seem reasonable because the more soil mass initially present in the fireball the less energy there will be available to heat water and air. The most important information from these results is that a significant change in the initial soil mass does not cause a significant change in the stabilized cloud top altitude and volume. Therefore a large error in the initial soil mass of the fireball will not necessary result in a large error in the predicted stabilized cloud top altitude and volume.

The 1 Mt case was repeated with the revised CRM. The stabilized cloud top altitude only changed by 0.8 of a percent from the value found with half the normal initial soil mass to the value found with twice the normal initial soil mass. The stabilized cloud volume was found to change by 9.0 percent for this case. These results are comparable to the results found with the original CRM, so the this study was carried no further.

Table VI. Comparing the Effect of Changing the Initial Soil Mass on the Stabilized Cloud Top Altitude

Yield (Kt)	Amount of Normal Initial Soil Mass	Top Alt. for Soil Mass (m)	Top Alt. for Normal Soil Mass (m)	Percent Change in Cloud Top
1.0	2.0	3147.	3212.	-2.0
1.0	0.5	3224.	3212.	0.4
10.0	2.0	6483.	6677.	-2.9
10.0	0.5	6731.	6677.	0.8
100.0	2.0	11710.	11960.	-2.1
100.0	0.5	12020.	11960.	0.5
1000.0	2.0	17970.	18150.	-1.0
1000.0	0.5	18160.	18150.	0.06
10000.0	2.0	31670.	31840.	-0.5
10000.0	0.5	31780.	31840.	-0.2
20000.0	2.0	42520.	42790.	-0.6
20000.0	0.5	42170.	42790.	-1.4

Table VII. Comparing the Effect of Changing the Initial Soil Mass on the Stabilized Cloud Volume

Yield (Kt)	Amount of Normal Initial Soil Mass	Cloud Vol. for Soil Mass (m)	Cloud Vol. for Normal Soil Mass (m)	Percent Change in Cloud Top
1.0	2.0	1.77E9	1.98E9	-10.6
1.0	0.5	2.09E9	1.98E9	5.6
10.0	2.0	1.14E10	1.45E10	-21.4
10.0	0.5	1.51E10	1.45E10	4.1
100.0	2.0	2.30E11	2.54E11	-9.4
100.0	0.5	2.62E11	2.54E11	3.1
1000.0	2.0	4.11E12	4.44E12	-7.4
1000.0	0.5	4.53E12	4.44E12	2.0
10000.0	2.0	5.57E13	5.89E13	-5.4
10000.0	0.5	5.98E13	5.89E13	1.5
20000.0	2.0	1.62E14	1.73E14	-6.4
20000.0	0.5	1.72E14	1.73E14	-0.6

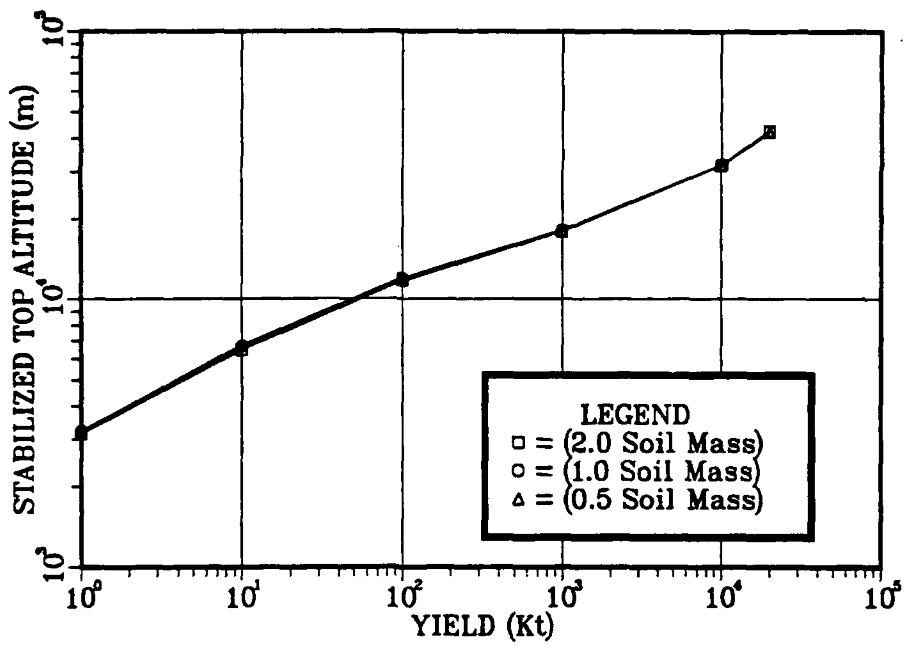

Figure 9. The Effect of Varying the Initial Soil Mass on the Stabilized Cloud Top Altitude - Original CRM

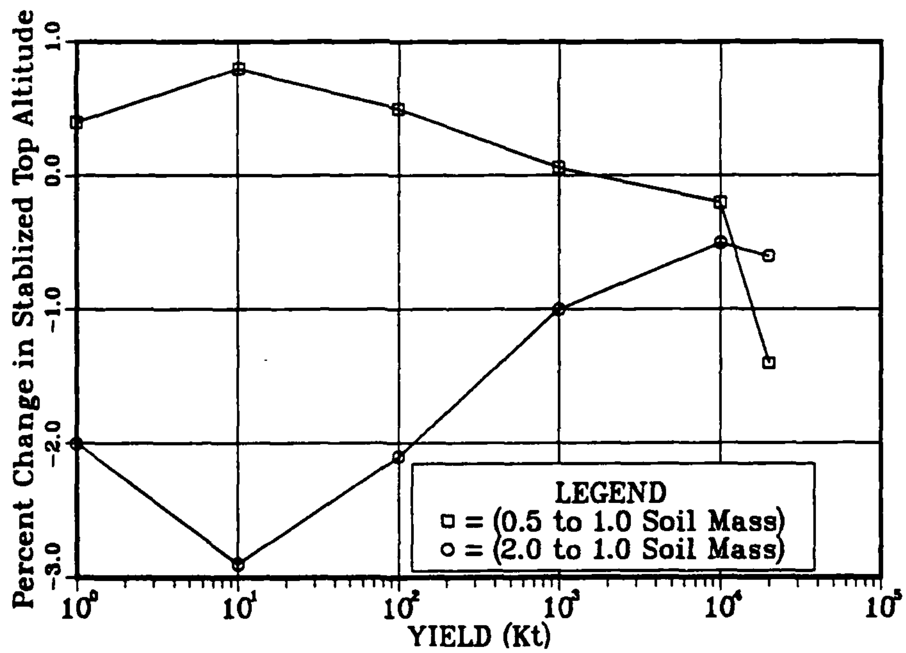

Figure 10. Comparing the Effect of Changing the Initial Soil Mass on the Stabilized Cloud Top Altitude - Original CRM

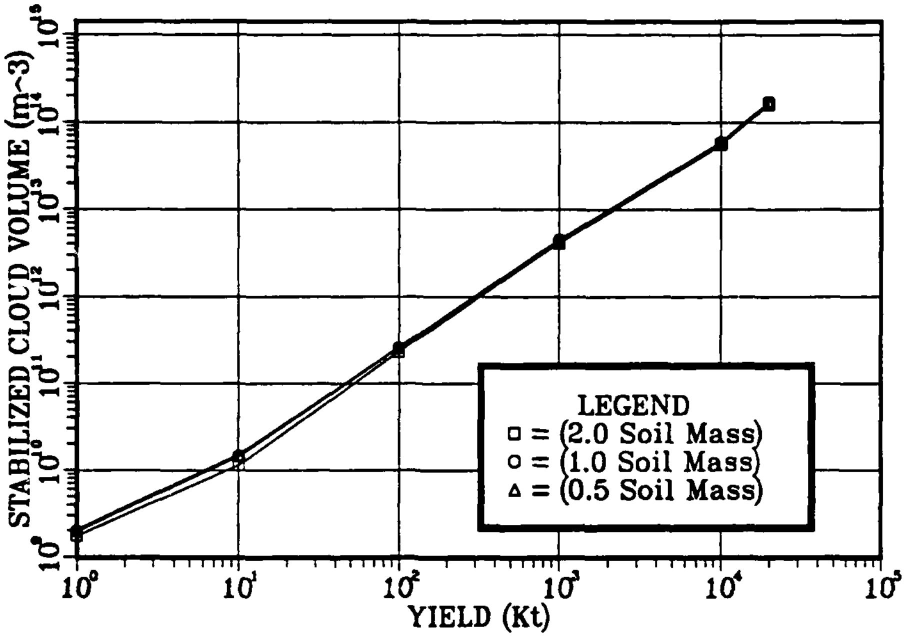

Figure 11. The Effect of Varying the Initial Soil Mass on the Stabilized Cloud Volume - Original CRM

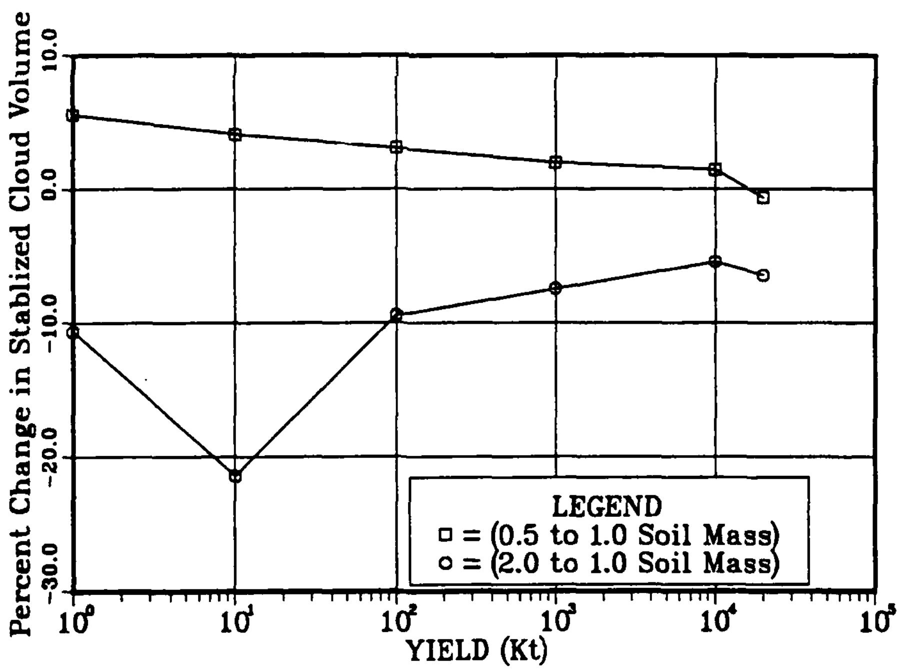

Figure 12. Comparing the Effect of Changing the Initial Soil Mass on the Stabilized Cloud Volume - Original CRM

Other Problems with the CRM

Some of the fundamental principles the CRM is based upon are very questionable. The limitations these assumptions place on the CRM predictions need to be studied and understood. After these assumptions are understood then it may be possible to improve the CRM of DELFIC further.

The differential equation describing how the cloud's temperature changes with time is based on an enthalpy balance, assuming the entrainment is a constant pressure process (5:5). The vertical extent of the cloud, especially for large yields, is such that the atmospheric pressure surrounding the cloud changes substantially from its base altitude to its top altitude. Therefore, the assumption of the entrainment being a constant pressure process is very questionable since the cloud is assumed to be in pressure equilibrium with the atmosphere (3:9).

The atmospheric data used by the coupled differential equations of the CRM are taken at the geometric cloud center altitude (4:43). This is a simplistic approach to supplying the atmospheric data needed by the CRM for its calculations. For large yields this technique is especially questionable.

The properties of the cloud are assumed to be

homogeneous and to have the values computed for the cloud center (4:43). Because of the dramatic torrodial nature of the cloud, this assumption seems fairly reasonable, especially for early times after the detonation and smaller yields. For higher yields at times near horizontal stabilization this representation of the cloud's properties may become inaccurate.

All of these questionable areas of the CRM deserve further consideration. They were not addressed in this study of the CRM. Once these questionable areas have been studied and understood it will be possible to make any necessary corrections and to know the actual limitations of the CRM.

Conclusions

The changes made to CRM of DELFIC corrected the way it handles atmospheric water vapor and surface water entrained by the cloud. Comparing how each version of the CRM handles atmospheric water vapor and surface water content shows clearly that the revised CRM models these effects more correctly.

The effect of increasing the amount of atmospheric water vapor was found to increase both the stabilized cloud top altitude and volume for each version of the CRM. The atmospheric water vapor entrained by the cloud will stay in the cloud until it condenses and falls out of the cloud. The latent heat of vaporization of the water vapor is given to the cloud when it condenses, resulting in the energy of the cloud being increased. This added energy to the cloud results in it taking longer to reach stabilization, giving it more time to rise and entrain air. Therefore, it is expected that as more atmospheric water is added the stabilized cloud top altitude and volume should increase. This general trend was followed by both versions of the CRM.

The energy contained in the cloud used to entrain surface water reduces the energy it has available to entrain air, water vapor, and soil. As more surface water mass is

entrained by the cloud the less dry air and atmospheric water vapor mass it is able to entrain. Therefore, as the amount of surface water present in the cloud increases, its density will also increase. The increase in the cloud's density will mean that more energy will be required to raise the cloud to a given altitude, resulting in it having a lower height of stabilization. Because the majority of the surface water present in the cloud will fallout before it reaches stabilization, the volume of the stabilized cloud will decrease as more surface water is added to it. Therefore, the result of increasing the amount of surface water mass contained in the cloud should be the stabilized cloud top altitude becoming lower and its volume smaller. For both versions of the CRM with yields less than 1 Mt, as the initial surface water mass is increased, their stabilized volume becomes smaller. For yields greater than 1 Mt, the revised CRM continues this trend, but the original CRM reverses it. Only for the revised version of the CRM does the cloud stabilized top altitude become lower as the initial surface water mass is increased; for the original CRM the stabilized top altitude becomes higher. Therefore, the revised version of the CRM models the cloud rise more realistically, especially with respect to the effect of initial surface water content.

The effect of significantly changing the amount of soil present in the cloud did not change drastically the predictions of either version of the CRM. Therefore, a significant error in the predicted amount of soil in the cloud will not necessarily result in a large error in the predictions of the CRM.

To further improve the revised CRM a more accurate distribution for the condensed water droplets in the cloud is required. This will not drastically change the results obtained, but it will make the condensed water fallout rate more valid. Also, further studies of the CRM are required to evaluate the other potential problems mentioned in the last section.

Appendix A: A Listing of the Changes Made to the CRM

The corrections made to the subroutines of the CRM were accomplished using the NOS Update Utility. This is a summary of those changes.

The error in the differential equation for momentum was corrected by replacing the old definition of the variable QQ in the DERIV subroutine on line 95 with:

```
QQ = QT * QX * QXE * RMIX
```

The error in the differential equation for turbulent kinetic energy was also corrected by this change.

The error in the differential equation for temperature for the dry case was corrected by first creating CPI:

$$CPI = \int_{T_e}^{T} C_p(T)dT$$

This was accomplished by inserting after line 54 in the DERIV subroutine the equation to create CPI:

```
CPI = (CPAI + X*(1697.66*(T - TE) + (1.14417/2.0)

        * (T**2.0 - TE**2.0))) / (1.0 + X)
```

The correction to the source code of (dT/dt) for the dry case was then made by replacing the variable CPAI in its equation with CPI. This was accomplished by deleting line 132 in the DERIV subroutine and replacing it with:

```
DT = -(RMIX*(QT*QX*QXE*9.8*U - EPS) + CPI*DRME/RM)/CR
```

The same problem existed in the differential equation describing the rate of change of the mass entrained by the cloud for the dry case, and it was also solved by replacing CPAI in its equation by CPI. Also it had an error in its source code (see page 14). Both of these problems were corrected by deleting line 117 of the DERIV subroutine and replacing it with:

```
100 DRM = (RM/(1.0 - RMIX*CPI/(CR*T*QX)))*RMIX*(RS*RL + (QT

           *QX*QXE*9.8*U - EPS)*
```

To correct the differential equation for the cloud's mass for the wet case a method for finding $P_w(t)$ needed to be created. To accomplish this a number of changes were made to the source code. First, after line 25 of the DERIV subroutine the following was inserted:

```
REAL CPI,DIAMW,VIS,DWP,FWP,NWP,PWF
```

This was to declare the new variables needed for creating $P_w(t)$, also CPI was included. These variables represent:

- DIAMW = the diameter of the water particles in the cloud (m)
- VIS = dynamic viscosity of the cloud gas (kg/m*sec)
- DWP = density of water particles = 1000 kg/m^3
- FWP = the calculated fall rate of the water particles (m/sec)
- NWP = $n_w(t)$
- PWF = $P_w(t)$

Then $P_w(t)$ was created by inserting after line 109 of the DERIV subroutine the following:

```
DIAMW = 100.0
VIS = (1.458E-6)*(T**1.5)/(110.4 + T)
DWP = 1000.0
CALL FALRT(DIAMW,DWP,Z,RA,VIS,FWP,ISOUT)
DIAMW=(1.0E-6)*DIAMW
NWP=((WT*RM)/(1.0+X+S+WT))*(1.9098593/(DWP*DIAMW**3.0))/V
PWF= 3.141527*(R**2.0)*DWP*FWP*(0.5235988)*(DIAMW**3.0)*NWP
```

The reason for DIAMW being initially defined as 100.0 is because the FALRT subroutine requires the diameter of the particles in micrometers. After the FALRT subroutine the value of DIAMW is converted back to meters. The problem with the equation for (dm/dt) for the wet case is then fixed by deleting line 164 of the DERIV subroutine and replacing it with:

```
     DRM = DRM - CMLR - PWF
```

The problem with the equation for calculating   for cases were N_d is greater than 140.0 and less than 4.5E7 was corrected by deleting lines 22 and 23 in the FALRT subroutine and replacing them with:

```
QLOGA = ALOG10(CDRR)
FALV = (VIS/(DEN*(1.0E-6)*DIAM))*10.0**(-1.29536
        + 0.986*QLOGA - 0.046677*QLOGA**2.0
        0.0011235*QLOGA**3.0)
```

The criteria of N_d = 140 for this case was changed to N_d = 100 by deleting line 18 of the FALRT subroutine and replacing it with:

```
     IF (CDRR.GT.100.0) GO TO 1
```

The problem with the differential equation for the soil mixing ratio in the cloud was fixed by deleting line 194 of the DERIV subroutine and replacing it with:

```
DS = -((1.0+X+S+WT)/RM)*(CMLR + S*DRME/(1.0 + XE))
```

The problem with the differential equation for the water mixing ratio in the cloud was fixed by deleting line 176 of the DERIV subroutine and replacing it with:

```
DWT = -((1.0+X+S+WT)/RM)*((WT+X-XE)/(1.0+XE)*DRME +PWF) - DX
```

The changes shown in this Appendix are all the changes made to the CRM of DELFIC to correct the problems mentioned in Section II. No other changes were made to the CRM.

Appendix B: The C Program Source Code used to Calculate the Initial Masses of Air, Water, and Soil in the Cloud

```
#include "df0:c/math.h"
#include "df0:c/stdio.h"

TI (W)
   double W;
      {
         double  x, n, K, c;

         n = (-0.4473)*pow( W, 0.0436 );
         K = (5980.0)*pow( W, -0.0395 );
         c = (56.0)*pow( W, -0.30 );

         x = K * pow( c, n) + 1500.0;
         return ( x ) ;
      }


Cs( Ti, Te )
   double Ti, Te;
      {
         double  x;

         x = 0.0;

         if ( Ti > 848.0 )
            {
               x = 1003.8*( Ti - 848.0 ) + (0.1351/2.0)*
                  ( Ti*Ti - 848.0*848.0 );
               Ti = 848.0;
            }
         x = x + 781.6*(Ti - Te) + (0.5612/2.0)*(Ti*Ti -
             Te*Te) + (1.881e7)*( 1.0/Ti - 1.0/Te );

         return ( x );
      }


Cpa( Ti, Te )
   double Ti, Te;
      {
         double x;

         x = 0.0;
```

```
        if ( Ti > 2300.0 )
           {
              x = -3587.5*( Ti - 2300.0) + (2.125/2.0)*
                  ( Ti*Ti - 2300.0*2300.0 );
              Ti = 2300.0;
           }
        x = x + 946.6*(Ti - Te) + (0.1971/2.0)*(Ti*Ti -
            Te*Te);
        return ( x );
     }


Cpw( Ti, Te)
   double Ti,Te;
     {
        double x;

        x = 1697.66*(Ti - Te) + (1.144174/2.0)*(Ti*Ti -
            Te*Te);
        return ( x );
     }


PWS( Te )
   double Te;
     {
        double x;

        x = 611.0 * pow( (273.0/Te), 5.13 ) * exp( 25.0*
            (Te - 273.0)/Te ) ;
        return ( x );
     }



main( )
   {
     double  H, Mi, Hr, Te, W, PHI, Tvi, x, P, Ti, Ms, Tsi,
             Pws, E, xe, L, Mai, Mwi, Vi;

     printf ("Enter the weapon yield (Kt).\n");
     scanf  ("%lf", &W);
     printf ("Enter the value of PHI.\n");
     scanf  ("%lf", &PHI);

     Hr = 0.0;
     Te = 295.0;
     P = 1.01325e5;

     Ti = TI ( W );
```

```
Ms = (0.07741) * pow( W, (3.0/3.4) ) *
     (180.0)*(180.0)*(360.0);
Tsi = ( 200.0 * log10( W ) + 1000.0 );
H = (0.45)*(4.18e12)*W;
Pws = PWS ( Te );
E = (29.0/18.0);
xe = (Hr * Pws)/(E*P);

if ( Te < 273.0 )
   L = 5.13e6;
else
   L = 2.5e6;

Mai = PHI*( H - Ms*Cs(Tsi,Te) ) / ( Cpa(Ti,Te) +
         xe*Cpw(Ti,Te) );

Mwi = ( 1.0 - PHI )*( H - Ms*Cs(Tsi,Te) ) /
        ( Cpw(Ti,Te) + L) + xe*Mai;

x = (Mwi/ Mai);
Tvi = Ti * ( 1.0 + x/E ) / ( 1.0 + x );

Mi = Mai + Ms + Mwi;
Vi = (Mai + Mwi) * (287.0) * Tvi / P;

printf ("Ms  = %.3e (kg)\n", Ms);
printf ("Mai = %.3e (kg)\n", Mai);
printf ("Mwi = %.3e (kg)\n", Mwi);
printf ("Mi  = %.3e (kg)\n", Mi);
printf ("Vi  = %.3e (m^3)\n", Vi);

}
```

Appendix C: The Effect of Atmospheric Water Vapor on the Original CRM

The original version of the CRM was examined to see how atmospheric water vapor affects cloud height and volume. These results were then compared to the results of the revised CRM. Three different atmospheric profiles were used to study the effect of atmospheric humidity on these versions of the CRM. These profiles contain atmospheric data such as temperature, air density, pressure, relative humidity, and viscosity at incremented altitudes. The atmospheric profile specified by the user is then used by the CRM in its calculations. The first atmospheric profile used was the U.S. Standard Atmosphere Mid Latitude Spring / Fall, MIDLSF, which is an averaged middle latitude spring-fall profile. The second atmospheric profile used was the MIDLSF profile with no relative humidity present at any altitude. This profile was referred to as the 0.0 Humidity profile. The last profile used was the Handbook of Geophysics (1965) Modified Tropic Atmosphere, TROPIC, which represents a tropical atmosphere with a high relative humidity content. These humidity profiles were used for runs of each version of the CRM for the following yields:

1kt, 10kt, 100kt, 1Mt, 5Mt, 10Mt, 15Mt, 20Mt.

The results found using the original CRM and the comparison of the results found with both versions of the CRM are shown in this Appendix. All of the results found for both versions of the CRM are discussed and compared in the section on "The Effect of Atmospheric Water Vapor on the CRM".

The stabilized top altitude and cloud volume for the MIDLSF and TROPIC profile results were compared to the result of the 0.0 Humidity Profile. These results for the original CRM are shown in Tables VIII and IX. Graphically, the stabilized cloud top data is shown in Figure 13, and a comparison of the results for the MIDLSF and TROPIC profiles verses the 0.0 Humidity profile is presented in Figure 14. The predicted volume of the stabilized cloud by the original CRM is shown Figure 15, and the change in the results found with the MIDLSF and TROPIC profiles compared to the 0.0 Humidity Profile result is shown in Figure 16.

The results found with each of the versions of the CRM were then compared directly to each other. The comparison of the stabilized cloud top data is presented in Table X, and the graphical representation of the results is shown in Figure 17. The comparison of the stabilized cloud volume

data is presented in Table XI, and the graphical representation of the results is shown in Figure 18.

Table VIII. Comparing Stabilized Cloud Top of the MIDLSF and TROPIC Profile Results to the 0.0 Humidity Profile Result - Original CRM.

Yield (Kt)	Humidity Profile	Profile Cloud Top (m)	0.0 Humidity Cloud Top (m)	Percent Change in Cloud Top
1.0	MIDLSF	3212.	3060.	5.0
1.0	TROPIC	2795.	3060.	-8.7
10.0	MIDLSF	6677.	6194.	7.8
10.0	TROPIC	6083.	6194.	-1.8
100.0	MIDLSF	11960.	11060.	8.1
100.0	TROPIC	14140.	11060.	27.8
1000.0	MIDLSF	18150.	17710.	2.5
1000.0	TROPIC	22330.	17710.	26.1
5000.0	MIDLSF	25720.	25390.	1.3
5000.0	TROPIC	29090.	25390.	14.6
10000.0	MIDLSF	31840.	31580.	0.8
10000.0	TROPIC	34760.	31580.	10.1
15000.0	MIDLSF	37610.	37010.	1.6
15000.0	TROPIC	40200.	37010.	8.6
20000.0	MIDLSF	42790.	42150.	1.5
20000.0	TROPIC	45050.	42150.	6.9

Table IX. Comparing Stabilized Cloud Volume of the MIDLSF and TROPIC Profile Results to the 0.0 Humidity Profile Result - Original CRM

Yield (Kt)	Humidity Profile	Profile Cloud Volume (m^3)	0.0 Humidity Cloud Volume (m^3)	Percent Change in Cloud Volume
1.0	MIDLSF	1.98E9	1.83E9	8.2
1.0	TROPIC	1.25E9	1.83E9	-31.7
10.0	MIDLSF	1.45E10	1.24E10	16.9
10.0	TROPIC	1.23E10	1.24E10	-0.8
100.0	MIDLSF	2.54E11	2.25E11	12.9
100.0	TROPIC	2.77E11	2.25E11	23.1
1000.0	MIDLSF	4.47E12	3.66E12	22.1
1000.0	TROPIC	5.60E12	3.66E12	53.0
5000.0	MIDLSF	2.53E13	2.51E13	0.8
5000.0	TROPIC	3.06E13	2.51E13	21.9
10000.0	MIDLSF	5.89E13	5.85E13	5.3
10000.0	TROPIC	6.91E13	5.85E13	18.1
15000.0	MIDLSF	1.08E14	1.03E14	4.9
15000.0	TROPIC	1.24E14	1.03E14	20.4
20000.0	MIDLSF	1.73E14	1.70E14	1.8
20000.0	TROPIC	1.86E14	1.70E14	9.4

Table X. Comparing Stabilied Cloud Top of the Original CRM to the Revised CRM for Different Humidity Profiles

Yield (Kt)	Humidity Profile	Original CRM Cloud Top (m)	Revised CRM Cloud Top (m)	Percent Change in Cloud Top
1.0	0.0	3060.	3086.	-0.8
1.0	MIDLSF	3212.	3182.	0.9
1.0	TROPIC	2795.	2743.	1.9
10.0	0.0	6194.	6297.	-1.6
10.0	MIDLSF	6677.	6628.	0.7
10.0	TROPIC	6083.	5986.	1.6
100.0	0.0	11060.	11230.	-1.5
100.0	MIDLSF	11960.	11980.	-0.1
100.0	TROPIC	14140.	13930.	2.1
1000.0	0.0	17710.	18020.	-1.7
1000.0	MIDLSF	18150.	18280.	-0.7
1000.0	TROPIC	22330.	22310.	0.1
5000.0	0.0	25390.	26300.	-3.5
5000.0	MIDLSF	25720.	26500.	-2.9
5000.0	TROPIC	29090.	29370.	-0.9
10000.0	0.0	31580.	33360.	-5.3
10000.0	MIDLSF	31840.	33560.	-5.1
10000.0	TROPIC	34760.	35560.	-2.2
15000.0	0.0	37010.	39870.	-7.2
15000.0	MIDLSF	37610.	40100.	-6.2
15000.0	TROPIC	40200.	41840.	-3.9
20000.0	0.0	42150.	46380.	-9.1
20000.0	MIDLSF	42790.	46650.	-8.3
20000.0	TROPIC	45050.	47970.	-6.1

Table XI. Comparing Stabilied Cloud Volume of the Original CRM to the Revised CRM for Different Humidity Profiles

Yield (Kt)	Humidity Profile	Original CRM Cloud Volume (m^3)	Revised CRM Cloud Volume (m^3)	Percent Change in Cloud Volume
1.0	0.0	1.83E9	1.820E9	0.5
1.0	MIDLSF	1.98E9	1.883E9	5.2
1.0	TROPIC	1.25E9	1.147E9	9.0
10.0	0.0	1.24E10	1.238E10	0.2
10.0	MIDLSF	1.45E10	1.246E10	16.4
10.0	TROPIC	1.23E10	1.029E10	19.5
100.0	0.0	2.25E11	2.211E11	1.8
100.0	MIDLSF	2.54E11	2.465E11	3.0
100.0	TROPIC	2.77E11	2.626E11	5.5
1000.0	0.0	3.66E12	3.927E12	-6.8
1000.0	MIDLSF	4.47E12	4.085E12	9.4
1000.0	TROPIC	5.60E12	5.503E12	1.8
5000.0	0.0	2.51E13	2.612E13	-3.9
5000.0	MIDLSF	2.53E13	2.335E13	8.4
5000.0	TROPIC	3.06E13	3.142E13	-2.6
10000.0	0.0	5.85E13	6.608E13	-11.5
10000.0	MIDLSF	5.89E13	6.604E13	-10.8
10000.0	TROPIC	6.91E13	7.452E13	-7.3
15000.0	0.0	1.03E14	1.274E14	-19.2
15000.0	MIDLSF	1.08E14	1.274E14	-15.2
15000.0	TROPIC	1.24E14	1.385E14	-10.5
20000.0	0.0	1.70E14	2.196E14	-22.6
20000.0	MIDLSF	1.73E14	2.209E14	-21.7
20000.0	TROPIC	1.86E14	2.252E14	-17.4

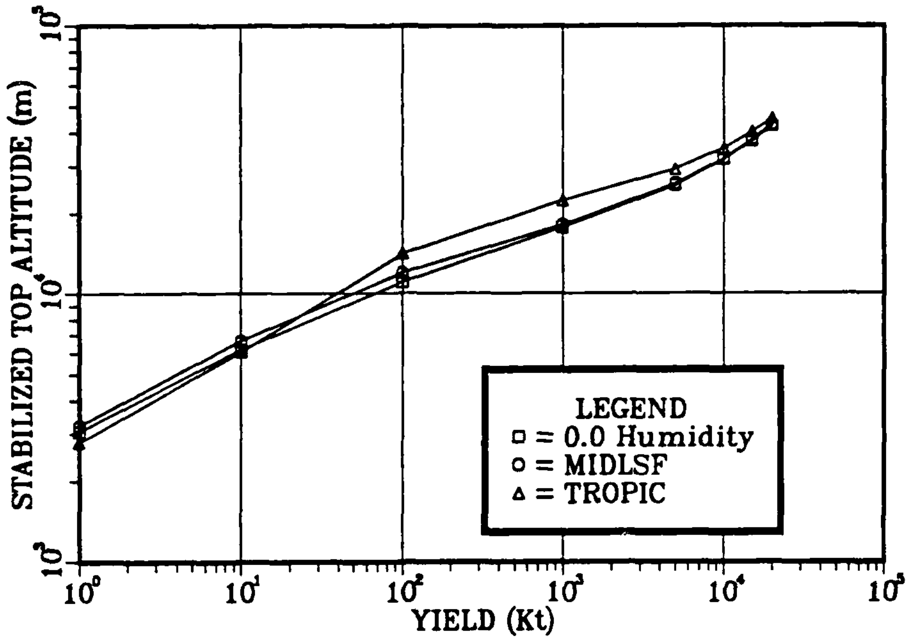

Figure 13. The Effect of Atmospheric Water Vapor on the Stabilized Cloud Top Altitude - Original CRM

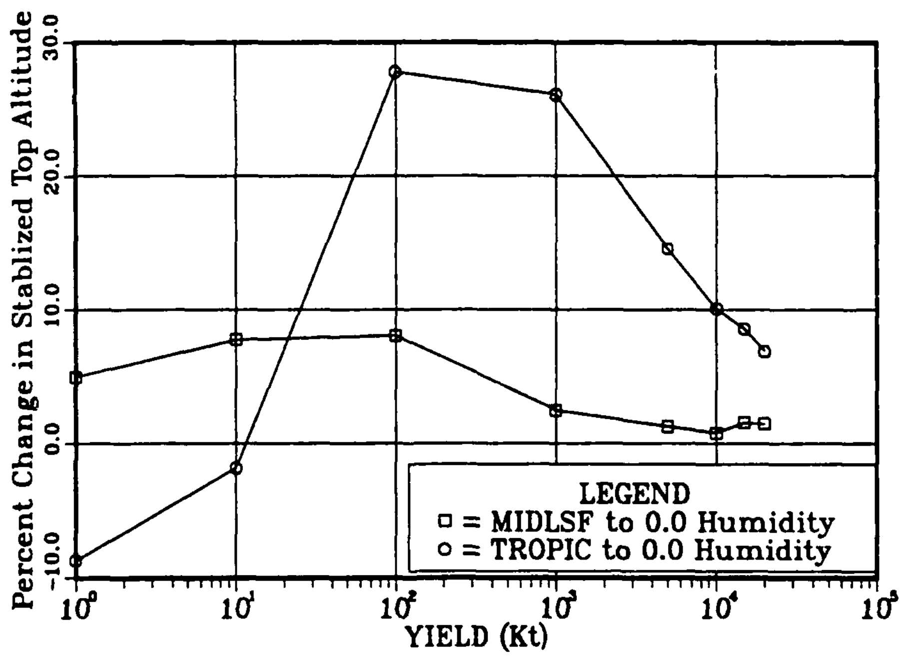

Figure 14. Comparing Stabilized Cloud Top of the MIDLSF and TROPIC Profile Results to the 0.0 Humidity Profile Result - Original CRM

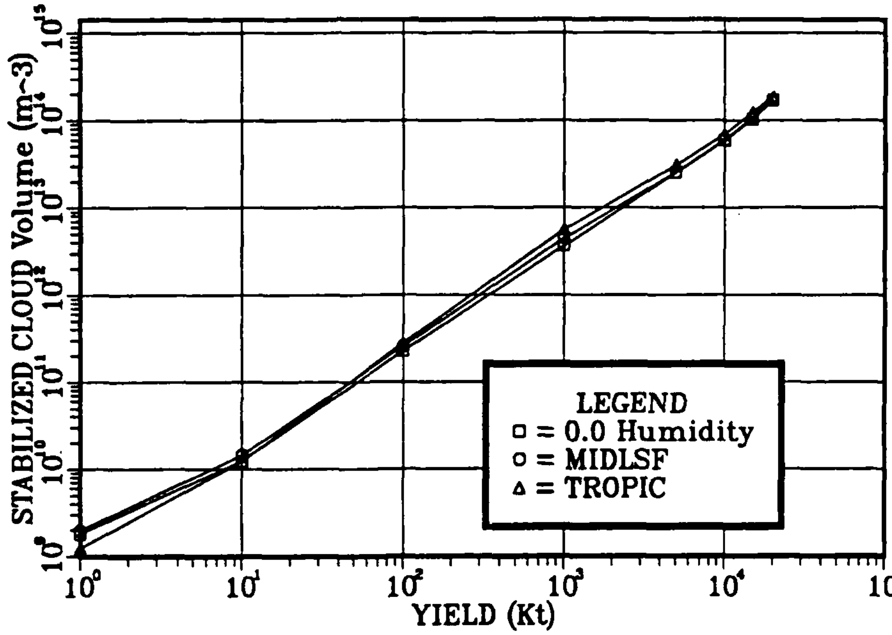

Figure 15. The Effect of Atmospheric Water Vapor on the Stabilized Cloud Volume - Original CRM

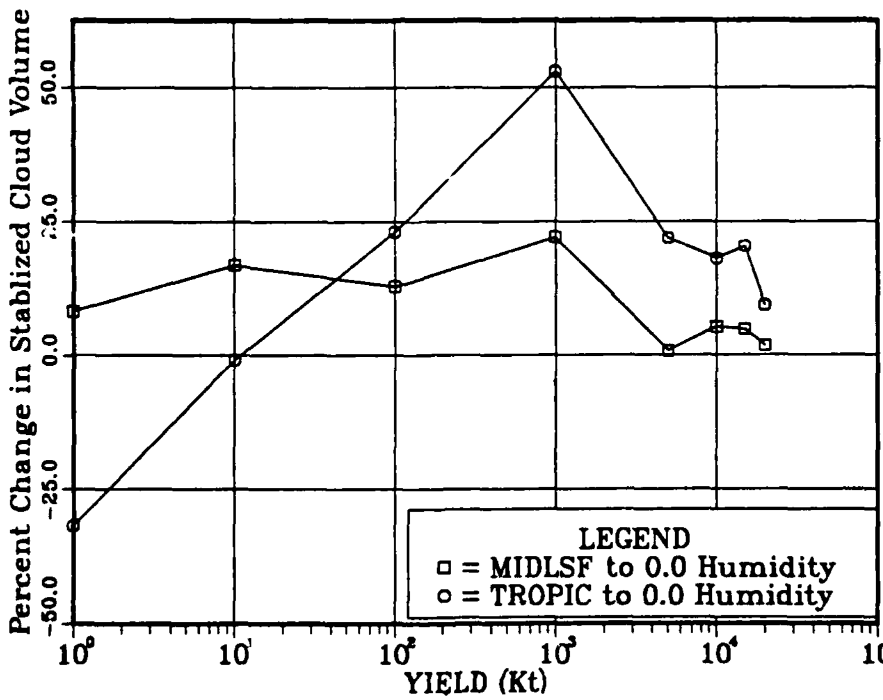

Figure 16. Comparing Stabilized Cloud Volume of the MIDLSF and TROPIC Profile Results to the 0.0 Humidity Profile Result - Original CRM

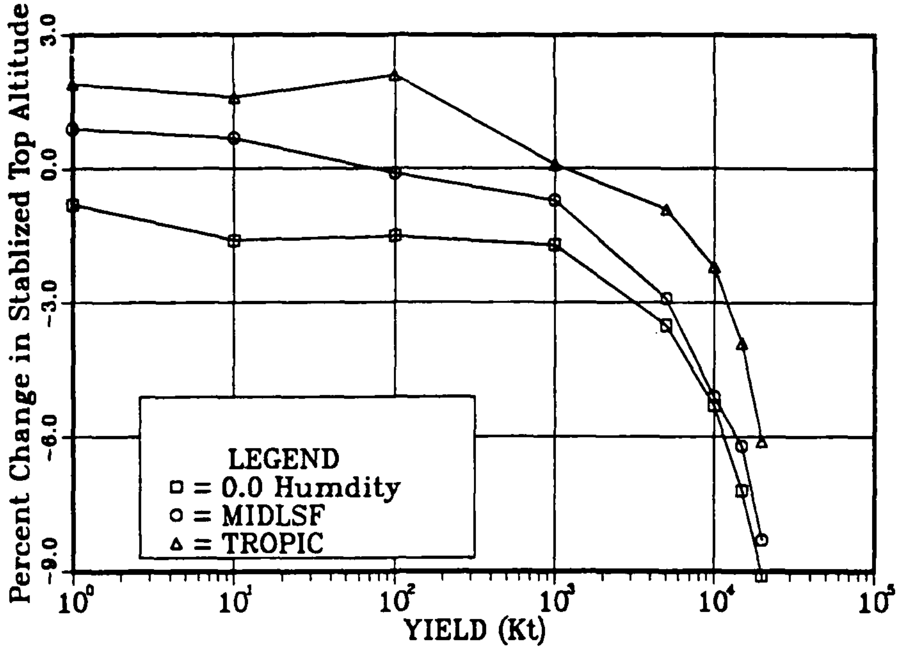

Figure 17. Comparing Stabilized Cloud Top of the Original CRM to the Revised CRM for Different Humidity Profiles

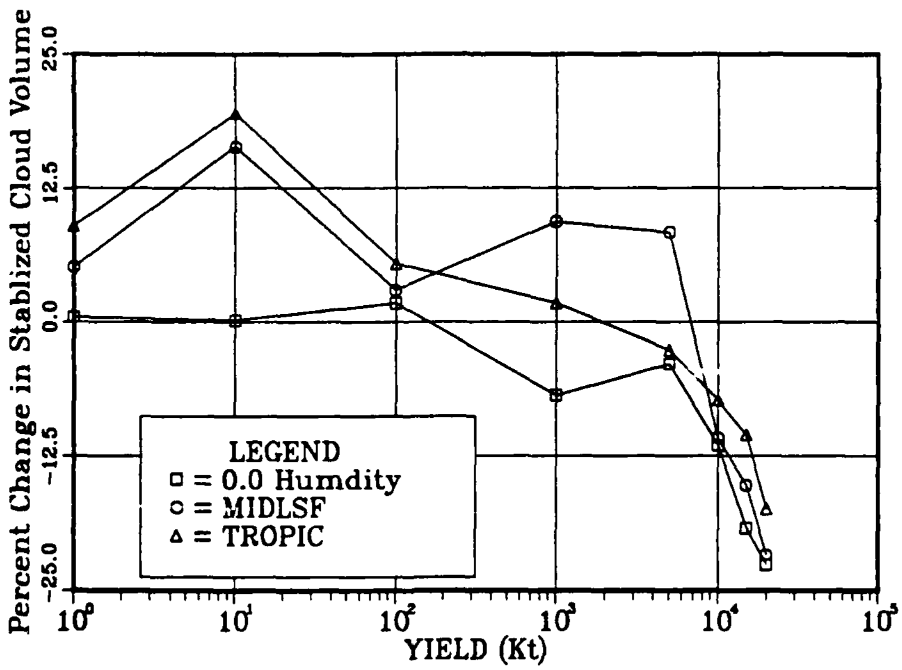

Figure 18. Comparing Stabilized Cloud Volume of the Original CRM to the Revised CRM for Different Humidity Profiles

Appendix D: The Effect of Surface Water on the Original CRM

The effect of changing the cloud surface water mass was examined for original version of the CRM. Then the results found using the original CRM were compared to the results of the revised CRM. The value of ϕ was varied to change the amount of initial water mass in the cloud. The 0.0 Humidity profile was used for all the cases examined, so all the water present in the cloud was from the surface water mass. Three values of ϕ were used: 1.0, 0.5, and 0.1. These values of ϕ were used for each of the following yields: 1kt, 10kt, 100kt, 1Mt, 5Mt, 10Mt, 15Mt, and 20Mt.

The results found using the original CRM and the comparison of the predictions of both versions of the CRM are presented in this Appendix. All of these results are discussed in the section on "The Effect of Surface Water on the CRM", and appropriate conclusions drawn.

The stabilized top altitude and cloud volume for $\phi = 0.5$ and $\phi = 0.1$ were first compared to values found with $\phi = 1.0$. The results found with the original CRM are shown in Tables XII and XIII. The predicted stabilized cloud top altitude is shown in Figure 19, and the

cloud volume is shown in Figure 21. The change in the cloud's stabilized top altitude for ϕ = 0.5 and ϕ = 0.1 compared to ϕ = 1.0 is shown graphically in Figure 20, and the change in the stabilized cloud volume in Figure 22.

The results found with each of the versions of the CRM were then compared directly to each other. The comparison of the stabilized cloud top data is presented in Table XIV, and the graphical representation of the results is shown in Figure 23. The comparison of the stabilized cloud volume data is presented in Table XV, and the graphical representation of the results is shown in Figure 24.

Table XII. Comparing Stabilized Cloud Top for $\phi = 0.5$ and $\phi = 0.1$ to the $\phi = 1.0$ Result - Original CRM

Yield (Kt)	ϕ	ϕ Cloud Top (m)	$\phi = 1.0$ Cloud Top (m)	Percent Change in Cloud Top
1.0	0.5	3043.	3060.	-0.6
1.0	0.1	3062.	3060.	0.07
10.0	0.5	6195.	6194.	0.02
10.0	0.1	6282.	6194.	1.4
100.0	0.5	11080.	11060.	0.2
100.0	0.1	11430.	11060.	3.3
1000.0	0.5	18060.	17710.	2.0
1000.0	0.1	18640.	17710.	5.3
5000.0	0.5	26600.	25390.	4.8
5000.0	0.1	28230.	25390.	11.2
10000.0	0.5	33860.	31580.	7.2
10000.0	0.1	37400.	31580.	18.4
15000.0	0.5	41300.	37010.	11.6
15000.0	0.1	------	------	----
20000.0	0.5	48920.	42150.	16.1
20000.0	0.1	------	------	----

Table XIII. Comparing Stabilized Cloud volume for Φ = 0.5 and Φ = 0.1 to the Φ = 1.0 Result - Original CRM

Yield (Kt)	Φ	Φ Cloud Volume (m^3)	Φ = 1.0 Cloud Volume (m^3)	Percent Change in Cloud Volume
1.0	0.5	1.68E9	1.83E9	-8.2
1.0	0.1	1.57E9	1.83E9	-14.2
10.0	0.5	1.15E10	1.24E10	-7.3
10.0	0.1	1.08E10	1.24E10	-12.9
100.0	0.5	2.09E11	2.25E11	-7.1
100.0	0.1	1.96E11	2.25E11	-12.9
1000.0	0.5	3.75E12	3.66E12	2.5
1000.0	0.1	3.96E12	3.66E12	8.2
5000.0	0.5	2.49E13	2.51E13	-0.8
5000.0	0.1	2.69E13	2.51E13	7.2
10000.0	0.5	6.24E13	5.85E13	6.7
10000.0	0.1	6.67E13	5.85E13	14.0
15000.0	0.5	1.25E14	1.03E14	21.4
15000.0	0.1	-------	1.03E14	----
20000.0	0.5	2.12E14	1.70E14	24.7
20000.0	0.1	-------	1.70E14	----

Table XIV. Comparing Stabilized Cloud Top of the Original CRM to the Revised CRM for Different Amounts of Surface Water Mass

Yield (Kt)	ϕ	Original CRM Cloud Top (m)	Revised CRM Cloud Top (m)	Percent Change in Cloud Top
1.0	1.0	3060.	3086.	-0.8
1.0	0.5	3043.	2899.	5.0
1.0	0.1	3062.	2730.	12.1
10.0	1.0	6194.	6297.	-1.6
10.0	0.5	6195.	5954.	4.0
10.0	0.1	6282.	5642.	11.3
100.0	1.0	11060.	11230.	-1.5
100.0	0.5	11080.	10620.	4.3
100.0	0.1	11430.	10080.	13.4
1000.0	1.0	17710.	18020.	-1.7
1000.0	0.5	18060.	17480.	3.3
1000.0	0.1	18640.	17120.	8.9
5000.0	1.0	25390.	26300.	-3.5
5000.0	0.5	26600.	25200.	5.6
5000.0	0.1	28230.	24580.	14.8
10000.0	1.0	31580.	33360.	-5.3
10000.0	0.5	33860.	31720.	6.7
10000.0	0.1	37400.	30690.	21.9
15000.0	1.0	37010.	39870.	-7.2
15000.0	0.5	41300.	37860.	9.1
15000.0	0.1	------	36510.	----
20000.0	1.0	42150.	46380.	-9.1
20000.0	0.5	48920.	43670.	12.0
20000.0	0.1	------	42000.	----

Table XV. Comparing Stabilized Cloud Volume of the Original CRM to the Revised CRM for Different Amounts of Surface Water Mass

Yield (Kt)	ϕ	Original CRM Cloud Volume (m^3)	Revised CRM Cloud Volume (m^3)	Percent Change in Cloud Volume
1.0	1.0	1.83E9	1.820E9	0.5
1.0	0.5	1.68E9	1.389E9	21.0
1.0	0.1	1.57E9	1.037E9	51.4
10.0	1.0	1.24E10	1.23E10	0.8
10.0	0.5	1.15E10	8.923E9	28.9
10.0	0.1	1.08E10	6.958E9	55.2
100.0	1.0	2.25E11	2.211E11	1.8
100.0	0.5	2.09E11	1.605E11	30.2
100.0	0.1	1.96E11	1.047E11	87.2
1000.0	1.0	3.66E12	3.927E12	-6.8
1000.0	0.5	3.75E12	3.079E12	21.8
1000.0	0.1	3.96E12	2.216E12	78.7
5000.0	1.0	2.51E13	2.612E13	-3.9
5000.0	0.5	2.49E13	2.109E13	18.1
5000.0	0.1	2.69E13	1.739E13	54.7
10000.0	1.0	5.85E13	6.608E13	-11.5
10000.0	0.5	6.24E13	5.081E13	22.8
10000.0	0.1	6.67E13	3.990E13	67.2
15000.0	1.0	1.03E14	1.274E14	-19.2
15000.0	0.5	1.25E14	9.536E13	31.1
15000.0	0.1	-------	7.436E13	-----
20000.0	1.0	1.70E14	2.196E14	-22.6
20000.0	0.5	2.12E14	1.589E14	33.4
20000.0	0.1	-------	1.216E14	-----

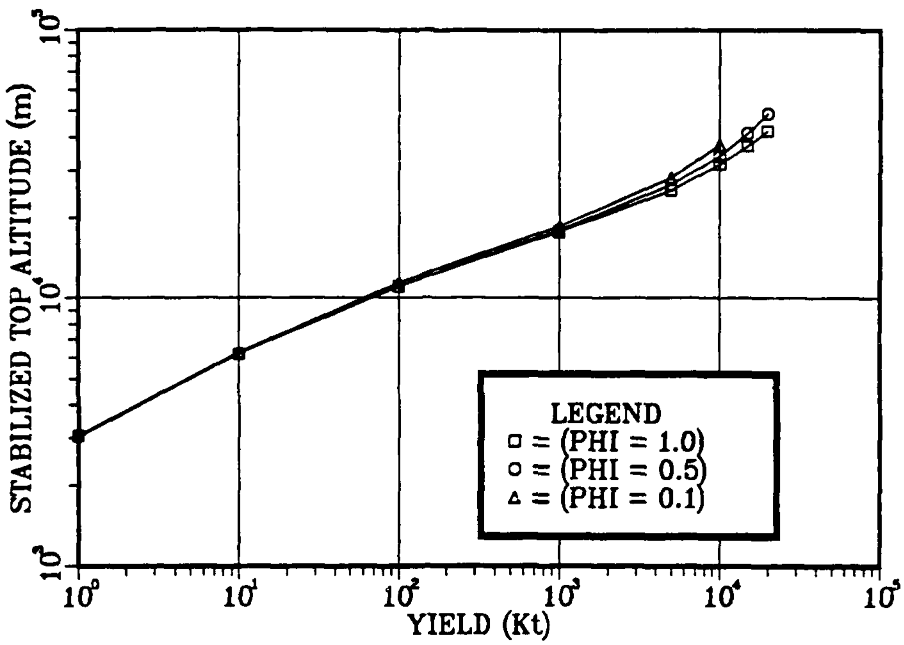

Figure 19. The Effect of Surface Water on the Stabilized Cloud Top Altitude - Original CRM

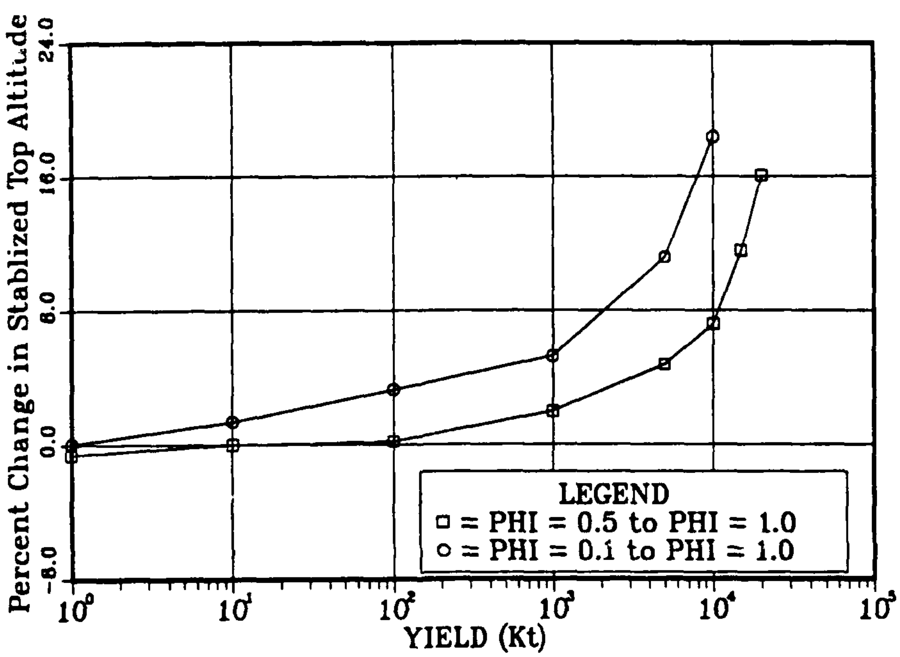

Figure 20. Comparing Stabilized Cloud Top for $\Phi = 0.5$ and $\phi = 0.1$ to the $\phi = 1.0$ Result - Original CRM

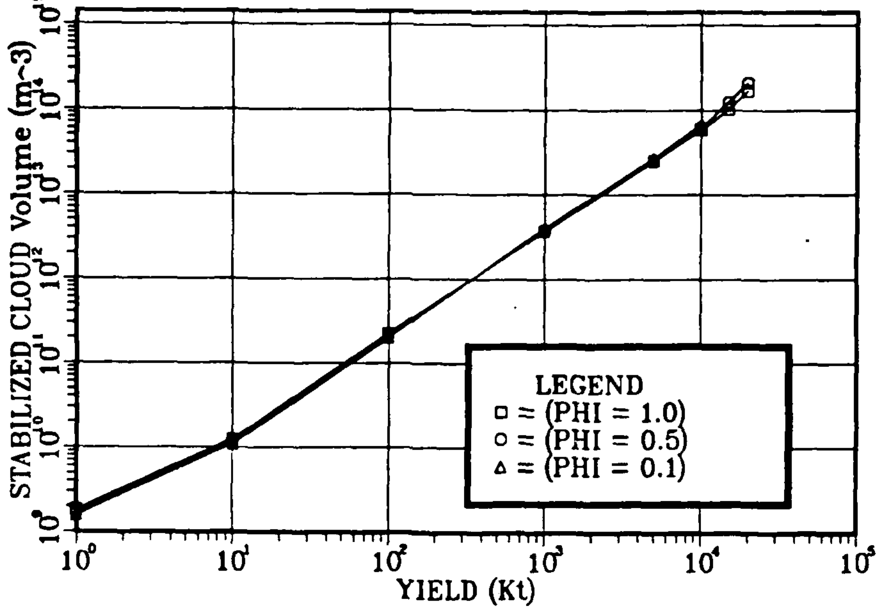

Figure 21. The Effect of Surface Water on the Stabilized Cloud Volume - Original CRM

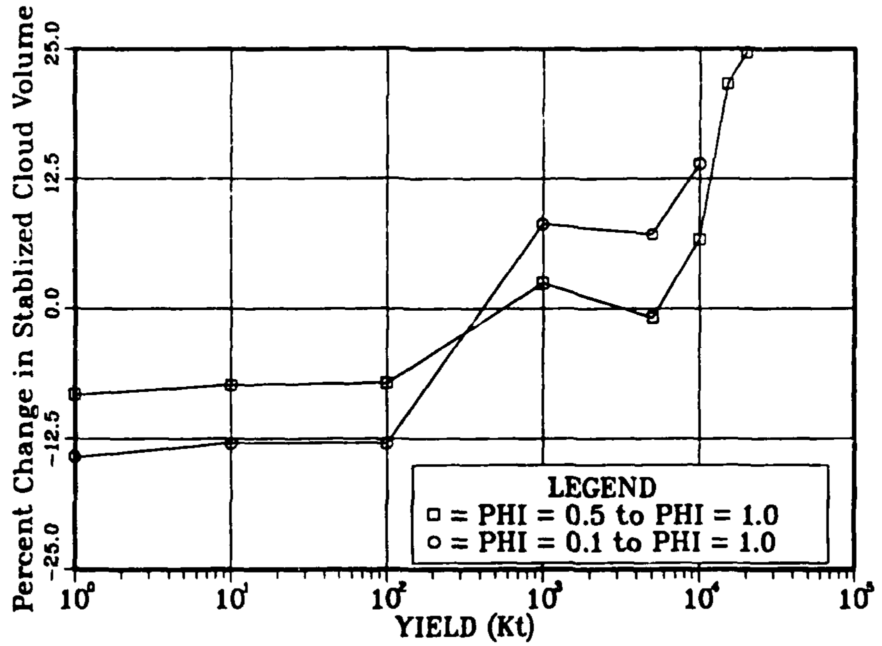

Figure 22. Comparing Stabilized Cloud Volume for = 0.5 and = 0.1 to the = 1.0 Result - Original CRM

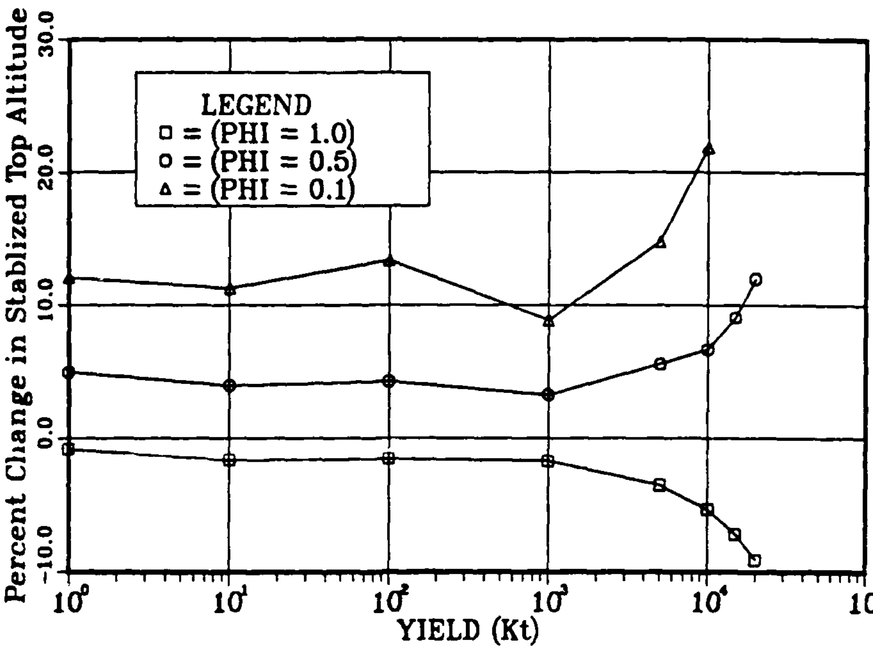

Figure 23. Comparing Stabilized Cloud Top of the Original CRM to the Revised CRM for Different Amounts of Surface Water Mass

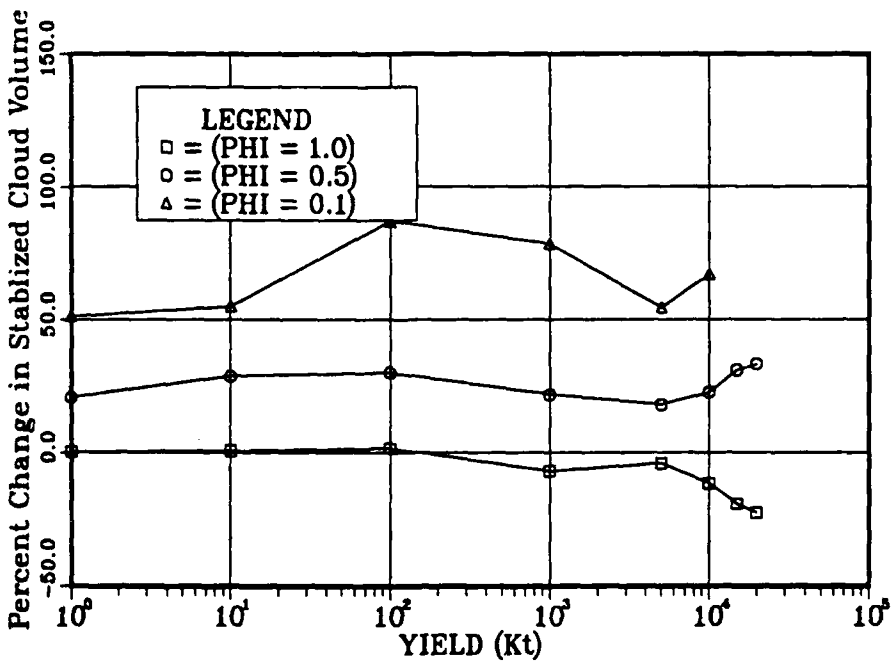

Figure 24. Comparing Stabilized Cloud Volume of the Original CRM to the Revised CRM for Different Amounts of Surface Water Mass

Bibilography

1. Davies, C. N. "Definitive Equations for the Fluid Resistance of Spheres," Physical Society of London, 57: 259-270 (1 July 1945).

2. Hewson, E. Wendell and Richmond W. Longley. Meteorology: Theoretical and Applied. New York: John Wiley & Sons, Inc., 19 .

3. Norment, Hillyer G. DELFIC: Department of Defense Fallout Prediction System, Volume I - Fundementals. Atmospheric Science Associates, DNA 5159F-1 (31 December 1979). AD-A088367

4. Norment, Hillyer G. Validation and Refinement of DELFIC Cloud Rise Module. Atmospheric Science Associates, DNA-4320F (15 January 1977). AD-A047 372

5. Norment, Hillyer G. and S. Woolf. Department of Defense Land Fallout Predictions System, Volume III - Cloud Rise (Revised), R70-1W. DASA-1800-III(Revised) (1 September 1970). AD-879 890

VITA

Second Lieutenant Bryan M. Minor was born on [redacted] in [redacted], at [redacted]. He graduated from Mount Vernon High School in Mount Vernon, Washington in 1982. Then he attended Central Washington University and received the degree of Bachelor of Science in Physics with minors in Math and Chemistry in June 1986. Upon graduation, he was commissioned in the USAF through the ROTC program. He then entered the School of Engineering,Air Force Institute of Technology, in August 1986.

Permanent address: [redacted]